HHS Public Access

Author manuscript

Nat Neurosci. Author manuscript; available in PMC 2024 November 01.

Published in final edited form as:

Nat Neurosci. 2024 May ; 27(5): 836–845. doi:10.1038/s41593-024-01599-2.

Pervasive environmental chemicals impair oligodendrocyte development

Erin F. Cohn[1], **Benjamin L.L. Clayton**[1], **Mayur Madhavan**[1], **Kristin A. Lee**[1], **Sara Yacoub**[1], **Yuriy Fedorov**[1], **Marissa A. Scavuzzo**[1], **Katie Paul-Friedman**[2], **Timothy J. Shafer**[2], **Paul J. Tesar**[1,*]

[1]Department of Genetics and Genome Sciences, Case Western Reserve University School of Medicine, Cleveland, Ohio 44106, USA

[2]Center for Computational Toxicology and Exposure, Office of Research and Development, U.S. Environmental Protection Agency, Research Triangle Park, North Carolina 27711, USA

Abstract

Exposure to environmental chemicals can impair neurodevelopment, and oligodendrocytes may be particularly vulnerable as their development extends from gestation into adulthood. However, few environmental chemicals have been assessed for potential risks to oligodendrocytes. Here, using a high-throughput developmental screen in cultured cells, we identified environmental chemicals in two classes that disrupt oligodendrocyte development through distinct mechanisms. Quaternary compounds, ubiquitous in disinfecting agents and personal care products, were potently and selectively cytotoxic to developing oligodendrocytes, whereas organophosphate flame retardants, commonly found in household items such as furniture and electronics, prematurely arrested oligodendrocyte maturation. Chemicals from each class impaired oligodendrocyte development postnatally in mice and in a human 3D organoid model of prenatal cortical development. Analysis of epidemiological data showed that adverse neurodevelopmental outcomes were associated with childhood exposure to the top organophosphate flame retardant identified by our screen. This work identifies toxicological vulnerabilities for oligodendrocyte development and highlights the need for deeper scrutiny of these compounds' impacts on human health.

* paul.tesar@case.edu .

AUTHOR CONTRIBUTIONS:

E.F.C., B.L.L.C., T.J.S., and P.J.T. conceived this study to screen effects of environmental chemicals on oligodendrocyte development. E.F.C., B.L.L.C., and P.J.T. designed and managed the experimental studies. E.F.C, B.L.L.C, K.A.L, and S.Y. performed, quantified, and analyzed in vitro experiments using mouse OPCs including primary screening, and immunocytochemistry. E.F.C., K.A.L., S.Y. performed dose-curve validations and qPCR. B.L.L.C. isolated mouse astrocytes and performed primary screening for astrocytes. E.F.C. performed RNA-seq analysis. E.F.C., K.A.L., and M.A.S. performed all in vivo experiments. K.P-F performed ToxPrint chemotype enrichment analyses and T.J.S. and K.P.F. guided categorization of chemical screen hits. E.F.C. designed and performed linear regression analyses using data from the National Health and Nutrition Examination Survey. M.M. and E.F.C. performed cortical organoid experiments. Y.F. managed the chemical library and pipelined primary screening data. E.F.C assembled all figures. E.F.C. and P.J.T. wrote the manuscript with input from all authors.

COMPETING INTERESTS:

The authors declare no competing interests related to this work.

MAIN:

Humans are exposed to a plethora of environmental chemicals, the majority of which have unknown toxicity profiles. However, chemical exposures alone may trigger pathogenesis or exacerbate underlying genetic factors to contribute to disease[1–3]. The developing central nervous system is particularly sensitive to environmental insults and chemical exposures can be especially harmful to children if they occur during critical periods of development[4,5]. For example, the heavy metals methylmercury and lead, as well as industrial chemicals such as polychlorinated biphenyls are known to disrupt brain development[6,7]. Importantly, the prevalence of neurodevelopmental disorders, including autism spectrum disorder and attention-deficit hyperactivity, has increased in the last decade[8,9]. However, genetic factors alone cannot fully account for this increase[4]. Therefore, evaluating how environmental factors, including chemical exposures, contribute to or initiate neurodevelopmental disorders has become imperative.

While neurons have been more thoroughly evaluated for their susceptibility to chemical toxicity[10,11], glial cells have been less studied in this context. Oligodendrocytes generate myelin to facilitate efficient neuronal transmission and provide metabolic and trophic support to neurons, which is essential for neuron function and longevity[12,13]. Conversely, impaired oligodendrocyte development or their loss results in significant cognitive and motor disability in genetic diseases such as Pelizaeus-Merzbacher disease, and in inflammatory diseases such as multiple sclerosis[14–16]. Both oligodendrogenesis and myelination have wide windows of vulnerability for environmental chemical exposure in humans. Development of oligodendrocytes from oligodendrocyte progenitor cells (OPCs) begins during fetal development and intensifies throughout the first two years of life. Once mature, oligodendrocytes will myelinate neurons, a process which peaks in infancy and childhood, but continues into adolescence and adulthood[17,18]. Therefore, oligodendrocytes are not only vulnerable during fetal development but also long after birth.

Few environmental chemicals including natural products and industrial compounds have been reported to specifically target oligodendrocyte function[19,20].The vast majority of chemicals present in the environment have not been evaluated for oligodendrocyte toxicity, in part due to prior challenges in capturing oligodendrocyte development at high purity and scale. In this study, we developed a toxicity screening platform to assess 1,823 chemicals that belong to the rapidly expanding repertoire of environmental contaminants. We identified chemicals belonging to two classes commonly found in households that perturb oligodendrocyte development.

RESULTS:

Environmental chemicals disrupt oligodendrocyte development

Previously, we established methods to generate OPCs from mouse pluripotent stem cells (mPSCs) at the scale required for high-throughput screening efforts[21–23]. mPSC-derived OPCs reliably develop into oligodendrocytes over 3 days *in vitro*, providing a robust approach for identifying environmental chemicals that affect oligodendrogenesis. We screened a library of 1,823 chemicals to assess their effects on development of OPCs

into oligodendrocytes (Fig. 1a). This library contains diverse chemicals with the potential for human exposure, including industrial chemicals, pesticides, and chemicals that are of interest to regulatory agencies[24]. In a primary screen, we treated OPCs with chemicals at a concentration of 20 μM and allowed oligodendrocytes to develop for 3 days before analysis. Toxicity screening during the OPC to oligodendrocyte developmental transition enabled us to identify both chemicals cytotoxic to developing oligodendrocytes and chemicals that impede oligodendrocyte generation without being cytotoxic.

We determined chemical cytotoxicity in oligodendrocytes by quantifying viable nuclei based on staining with 4′,6-diamidino-2-phenylindole (DAPI), and considered chemicals cytotoxic that reduced viability by more than 30% compared to the negative control. We further classified the remaining non-cytotoxic chemicals based on whether they interfered with the development of oligodendrocytes from OPCs by immunostaining for the O1 antigen, which is exclusively expressed on maturing oligodendrocytes. We considered non-cytotoxic chemicals that reduced the percentage of O1-positive cells by greater than 50% to be inhibitors of oligodendrocyte development. Conversely, we considered chemicals that increased the percentage of O1-positive cells by more than 22% to be drivers of oligodendrocyte development (Fig. 1b,c, and Extended Data Fig. 1a,b). Of the 1,823 chemicals in the primary screen, more than 80% had no effect on oligodendrocyte development or viability, 292 were identified as cytotoxic to developing oligodendrocytes, 47 inhibited oligodendrocyte generation, and 22 stimulated oligodendrocyte generation (Fig. 1b, and Supplementary Table 1).

Quaternary compounds are selectively cytotoxic to oligodendrocytes

To validate cytotoxic hits from the primary screen, we used a colorimetric MTS tetrazolium assay designed to assess cell viability by measuring metabolic activity (Fig. 1d). To identify chemicals with selective cytotoxicity to oligodendrocyte development, we compared cytotoxicity profiles of 206 MTS-validated chemicals from the primary screen to both an in-house primary screen in mouse astrocytes, representing another glial subtype, and a public database from the US Environmental Protection Agency (EPA), that contains cytotoxicity data for many cell types but not glial cells (Fig. 1e and Extended Data Fig. 1c,d). Chemicals cytotoxic to oligodendrocyte development but non-cytotoxic to astrocytes were tested in 10-point dose response (40 nM to 20 μM) and used to calculate IC_{50} values for each chemical (Fig. 1e). Finally, we ranked the top 10 cytotoxic chemicals based on potency in developing oligodendrocytes, lack of cytotoxicity to astrocytes, and lack of potency in cytotoxicity assays using other cell types (Fig. 1e).

Through computational analysis we identified a chemical structure, characterized by a central nitrogen with four alkyl groups (bond.quatN_alkyl_acylic), as the most enriched structural domain among chemicals cytotoxic specifically to oligodendrocytes. This bond defines 13 quaternary ammonium compounds in the 1,823 chemical library. The primary screen identified 9 of these chemicals as cytotoxic to oligodendrocyte development, 4 of which are found in the top 12 cytotoxic hits, including methyltrioctylammonium chloride (Fig. 1f,g, and Supplementary Table 2). The most highly ranked oligodendrocyte cytotoxic chemical, tributyltetradecylphosphonium (a quaternary phosphonium compound) has similar

structure and function to quaternary ammonium compounds[25]. Given that our primary screen and secondary validation assays utilized mPSC-derived oligodendrocytes, we next confirmed cytotoxicity for two of the top ranked cytotoxic hits on oligodendrocytes generated from primary OPCs isolated directly from mouse postnatal brain tissue. Both methyltrioctylammonium chloride and tributyltetradecylphosphonium chloride, the two most highly ranked quaternary ammonium and phosphonium compounds (quaternary compounds) were cytotoxic at 20 μM to primary OPCs, resulting in greater than 80% reduction in cell viability (Extended Data Fig. 2 a,b). To illustrate the specificity of quaternary compound induced cytotoxicity, we tested an expanded panel of quaternary compounds in astrocytes as well as a non-neural cell type, fibroblasts (Fig. 1h–k, Extended Data Fig. 2c–i). The additional quaternary compounds, cetylpyridinium chloride and alkyl (C12-C14) dimethylethylbenzyl ammonium chloride (ADEBC C12-C14), were selected for their high likelihood of human exposure due to their prevalence in common household products such as disinfecting agents[26–28]. Testing quaternary compounds in dose response demonstrated that all compounds were cytotoxic to astrocytes and fibroblasts only at concentrations 21-100 fold higher than those observed to be cytotoxic in developing oligodendrocytes (Fig 1h–k, Extended Data Fig. 2c–i). Collectively, these data demonstrate a toxicological sensitivity in developing oligodendrocytes to quaternary compound induced cytotoxicity.

Quaternary compounds activate the integrated stress response

To identify the mechanism underlying quaternary compound cytotoxicity in developing oligodendrocytes, we tested small molecule inhibitors of multiple programmed cell death pathways. We found that only QVD-OPH, an inhibitor of apoptosis, was able to prevent cell death induced by exposure to quaternary compounds (Extended Data Fig. 2j).

To determine the upstream signaling pathways responsible for triggering apoptosis, we performed RNA sequencing on developing oligodendrocytes treated for 4 hours with three quaternary compounds: methyltrioctylammonium chloride, cetylpyridinium chloride, and ADEBC (C12-C14) (Fig. 2a and Extended Data Fig. 2k,l). Gene set enrichment analysis (GSEA) revealed that quaternary compound exposure results in enrichment for hallmark gene sets involved in programmed cell death, the unfolded protein response, and the integrated stress response (ISR) (Fig. 2b,c, and Supplementary Table 3). The ISR is activated by diverse environmental stressors and if not resolved, can lead to cell death[29]. We confirmed quaternary compound induced ISR activation by performing qPCR for *Ddit3*, the gene that encodes C/EBP homologous protein (CHOP), as a canonical marker of ISR activation and mediator of ISR-induced apoptosis (Fig. 2d). Incubation of fibroblasts with quaternary compounds at multiple concentrations failed to elicit the same response in CHOP accumulation, suggesting that quaternary compound induced ISR activation may be specific to oligodendrocytes (Fig. 2d and Extended Data Fig. 2m,n). ISRIB, a small molecule inhibitor of the ISR, partially attenuated quaternary compound induced cell death, and acted with QVD-OPH synergistically to fully rescue cell viability (Fig. 2e). Small molecule inhibitors of NFkB and p53 signaling, two other enriched hallmark gene sets, did not increase cell viability (Extended Data Fig. 2o). These data suggest that quaternary compounds initiate ISR-mediated apoptosis specifically in developing oligodendrocytes.

We next sought to elucidate the effects of quaternary compounds on oligodendrocyte development *in vivo*; however, the ability of these chemicals to cross the blood brain barrier during the early postnatal period is not known. To determine whether quaternary compounds could penetrate the blood brain barrier postnatally, we administered methyltrioctylammonium chloride, cetylpyridinium chloride, and ADEBC (C12-C14) at doses of 10 and 100 mg/kg/day via oral gavage to mice from postnatal day 9 to 10. All three quaternary compounds successfully crossed the blood brain barrier, resulting in brain tissue concentrations in the nanomolar range (Extended Data Fig. 3a,b). We next evaluated the effects of administering cetylpyridinium chloride, the quaternary compound found at the highest concentration in brain tissue, for ten days from postnatal day 5 to 14, an essential period for oligodendrogenesis and myelination (Fig. 2f). Mice administered 10 mg/kg/day failed to survive the ten-day period (Extended Data Fig. 3c). Administration of 1 mg/kg/day resulted in nanomolar brain tissue concentration, which did not elicit changes in gross development including body, brain and liver weights (Fig. 2g and Extended Data Fig. 3d–g). Immunohistochemical analyses demonstrated significant depletion of SOX10+ oligodendrocyte lineage cells in multiple brain regions including the corpus callosum, cerebellum, cortex, and hippocampus (Fig. 2h,i and Extended Data Fig. 3h,i). The density of NeuN+ neurons was modestly reduced only in the cerebellum, suggesting that oligodendrocytes have enhanced sensitivity to quaternary compound toxicity *in vivo* (Extended Data Fig. 3j,k). These data show that quaternary compounds pose a risk specifically to oligodendrocytes during their postnatal development *in vivo*.

Quaternary compounds are cytotoxic to human oligodendrocyte development

To determine whether quaternary compounds could disrupt human oligodendrocyte development, we leveraged our human pluripotent stem cell (hPSC)-derived regionalized neural organoid model in which oligodendrogenesis and myelination are integrated with fundamental processes of prenatal cortical development[30,31]. We supplemented media with methyltrioctylammonium chloride, cetylpyridinium chloride, and ADEBC (C12-C14) for 10 days during a critical time period for oligodendrocyte development (Fig. 2j). Immunohistochemistry demonstrated that cell density was maintained across all conditions; however, we documented significant reductions in the density of SOX10+ OPCs and oligodendrocytes (Fig. 2k–m). Progenitor populations, including SOX2+SOX10+ “pre-OPCs” were preferentially reduced by quaternary compounds when compared to SOX2+SOX10− progenitors which increased in density (Extended Data Fig. 3l–n). Further analyses demonstrated that the number of NeuN+ neurons remained the same across all conditions (Extended Data Fig. 3l,o). These results demonstrate that quaternary compounds are selectively cytotoxic specifically to cells belonging to the human oligodendrocyte lineage in an *in vitro* model of early brain development.

Organophosphate flame retardants arrest oligodendrocyte development

Many toxicity screens evaluate cell viability as a single endpoint measure. However, our screening platform allowed us to both identify cytotoxic chemicals and evaluate whether non-cytotoxic chemicals affect an essential developmental transition. Of the 1,531 non-cytotoxic compounds identified in the primary screen, 69 altered oligodendrocyte development. The 22 chemicals identified as enhancers of oligodendrocyte

development included thyroid hormone receptor modulators which are well known to drive oligodendrocyte generation (Extended Data Fig. 4a)[32]. The remaining 47 chemicals inhibited oligodendrocyte development (Fig. 3a). Computational analysis of oligodendrocyte inhibitors revealed an enriched structure characterized by a central phosphate (bond.P.O_phosphate_alkyl_ester) as a top enriched structure with the highest odds ratio (Fig. 3b, and Supplementary Table 2). This structure is found in three chemical hits: tris(methylphenyl) phosphate (TMPP), tris(2,3-dibromopropyl) phosphate (TBPP), and tris(1,3-dichloro-2-propyl) phosphate (TDCIPP). These chemicals are all organophosphate esters that belong to a large class of compounds widely used as both pesticides and flame retardants (Fig. 3c, and Extended Data Fig. 4b). Of the 13 organophosphate flame retardants in the primary screen chemical library, 7 chemicals reduced the percentage of O1-positive oligodendrocytes. We tested the top 3 organophosphate flame retardants in 8-point dose response (30 nM to 20 μM) and used these data to generate IC_{50} values (Fig. 3d, and Extended Data Fig. 4b). All three organophosphate flame retardants also inhibited the development of oligodendrocytes from mouse OPCs isolated directly from postnatal brain tissue (Extended Data Fig. 4c,d).

In our toxicity screening platform, oligodendrocyte development proceeds through successive stages characterized by expression of known maturation markers (Fig. 3e). Specifically, early oligodendrocytes express the antigen for O4, intermediate oligodendrocytes express the antigen for O1, and mature oligodendrocytes express myelin basic protein (MBP). To identify the stage of oligodendrocyte maturation at which organophosphate flame retardants exert their effect, we cultured developing oligodendrocytes in the presence of TDCIPP, TMPP, and TBPP and assessed maturation over three days. When we assessed the effects of organophosphate flame retardants on oligodendrocyte generation using immunocytochemistry for early (O4+), intermediate (O1+), and mature (MBP+) oligodendrocytes, we detected a delay in acquisition of O4 expression, and decreased O1 and MBP expression relative to the vehicle (DMSO)-treated negative control at all time points (Fig. 3e–g, and Extended Data Fig. 4e,f). These results indicate that, mechanistically, organophosphate flame retardants arrest the initial progression of early oligodendrocytes to intermediate and mature oligodendrocytes.

TDCIPP impairs oligodendrocytes during mouse and human brain development

To evaluate the effects of early postnatal exposure to organophosphate flame retardants *in vivo*, we administered TDCIPP daily to mice via oral gavage at doses of 10 mg/kg/day or 100 mg/kg/day from postnatal days 5 to 14. No significant changes in body weight, brain or liver weight were detected in mice treated with TDCIPP (Extended Data Fig. 4g–i). TDCIPP was detected in brain as well as liver tissue (Fig. 3h and Extended Data Fig. 4j). At postnatal day 14, the number of SOX10+CC1+ oligodendrocytes was significantly reduced in multiple areas of the brains of mice treated with TDCIPP including the corpus callosum and cerebellum (Fig. 3i–k and Extended Data Fig.4k,l).

Next, we used our human cortical organoid model to assess whether organophosphate flame retardants inhibit human oligodendrocyte development. After culturing organoids from day 60 to day 70 in the presence of TDCIPP, we collected samples for immunohistochemistry.

In the presence of TDCIPP, overall cell density was not changed; however, SOX10+CC1+ oligodendrocytes were significantly decreased by more than 70% (Fig. 4a–c). SOX10+CC1− oligodendrocyte progenitors were also reduced, however by 30%, which may result from depletion of the OPC pool as oligodendrocytes fail to mature, or direct toxicity due to extended flame retardant exposure (Fig. 4a, d). We found that the density of NeuN+ neurons was unchanged across conditions, suggesting that the deficit in mature oligodendrocytes is indeed a selective inhibition of oligodendrocyte development (Extended Data Fig. 5a,b). Collectively, these results suggest that the presence of TDCIPP is sufficient to arrest human oligodendrocyte development.

TDCIPP exposure is significantly associated with abnormal neurodevelopment

Organophosphate flame retardants are widely used in common products including furniture, building materials, and electronics. Human epidemiological studies investigating potential links between exposure to organophosphate flame retardants and developmental neurotoxicity have largely focused on prenatal exposures[33]. However, given the prolonged period of oligodendrogenesis and myelination after birth, we asked whether postnatal neurodevelopment would be impacted by organophosphate flame retardant exposure throughout childhood and adolescence. To that end, we analyzed data from the US CDC's National Health and Nutrition Examination Survey (NHANES) to identify levels of childhood exposure to organophosphate flame retardants and associations between exposure and indicators of abnormal cognitive and motor development. The NHANES is a cross-sectional study designed to collect survey, laboratory, and examination data from a nationally representative sample of US children and adults. Due to the complex study design, these data can be leveraged to make estimations, including associations between laboratory-measured exposures and adverse outcomes, that are representative to the entire US population.

Previous work has shown that the urine metabolite bis(1,3-dichloro-2-propy) phosphate (BDCIPP) can accurately estimate exposure to its parent compound, the organophosphate flame retardant TDCIPP[34]. In examining a population of US children 3-11 years of age surveyed between 2013 and 2018, we found that BDCIPP was present in urine samples for 1,753 out of 1,763 (or 99.4%) of children (Fig. 4e). Additionally, the amount of creatinine-adjusted BDCIPP in children was significantly higher when compared to adults (Fig. 4f), suggesting that children may experience higher internal flame retardant doses. Comparing BDCIPP levels across data cycles demonstrates that childhood exposure to organophosphate flame retardants may be increasing (Fig. 4g).

To identify associations between organophosphate flame retardant exposure and abnormal neurodevelopment we examined levels of urinary BDCIPP in children 3-11 years of age and their associations with two neurodevelopmental measures: gross motor dysfunction and a need for special education (Fig. 4h and Extended Data Fig. 5c). These outcomes have been previously used to evaluate neurocognitive and neuromotor function[35,36] and depend on successful oligodendrocyte development as oligodendrogenesis and myelination play essential roles in memory, learning, and motor function[37–39]. We found that a larger proportion of children in the US who needed special education or reported having motor

dysfunction fell within the highest quartile of urinary BDCIPP concentration (Fig. 4i). Using multivariable-adjusted logistic regression, we identified significant associations between high levels of urinary BDCIPP, and both neurodevelopmental measures (Fig 4.j). Weighted logistic regression analyses accounted for the NHANES complex survey design and were adjusted for age, sex, race/ethnicity, urine creatinine, as well as socioeconomic confounders previously reported to be associated with each outcome[35,36]. Children in the highest quartile of urinary BDCIPP concentration had increased adjusted odds ratios for both neurodevelopmental outcomes when compared to children in the lowest quartile of urine BDCIPP concentration. The fully adjusted odds ratios for children in the highest BDCIPP concentration group were 2.0 (95% CI = 1.0-3.8) for special education and 6.0 (95% CI = 1.7-21.9) for gross motor dysfunction (Fig. 4j and Extended Data Fig. 5d,e,). Children in the third quartile also had significantly increased odds for motor dysfunction with an odds ratio of 4.2 (95% CI = 1.1-16.2). Additional significant predictors for special education included age, gender, race, the educational level of the subject's household reference person, and prenatal smoke exposure (subject's mother smoked while pregnant) (Extended Data Fig. 5d,e). These results indicate that children with high exposure are between 2 and 6 times more likely to experience adverse neurodevelopmental outcomes, providing strong evidence of a positive association between organophosphate flame retardant exposure and abnormal neurodevelopment.

DISCUSSION:

Evaluation of chemical safety is essential for the protection of human health. Although the effects of the vast majority of environmental chemicals on the central nervous system are unknown, high throughput screening is a powerful tool to prioritize chemicals of concern and identify environmental triggers of pathogenesis based on their toxic effects to relevant neural cell types [2,40]. Because oligodendrocytes represent a unique and understudied cell population in developmental neurotoxicology, we developed a toxicity screening platform to interrogate 1,823 environmental chemicals for their effects on oligodendrocyte development. This platform was designed to efficiently identify potential neurotoxicants through our use of scalable, pure mouse OPCs, and by screening chemicals with unknown bioactivity. Our use of human cortical organoids to assess the risks of potential toxicants to human health equipped us to identify species-specific and conserved responses, and serves as an expansion on previous efforts utilizing other models for developmental neurotoxicity testing[20,41–43]. Through this approach, we identified chemicals from two classes that impede the generation of mouse and human oligodendrocytes: quaternary compounds and organophosphate flame retardants.

Quaternary compounds are common in personal care products, pharmaceuticals, and anti-static agents. The prevalent use of these chemicals in disinfectants, including more than half of EPA-registered products for eliminating SARS-CoV-2, is a likely cause of increased human exposure, demonstrated by the doubling in blood levels of some quaternary ammonium compounds since before the COVID-19 pandemic[44,45]. In our oligodendrocyte-specific cytotoxic hits, quaternary compounds as a class were enriched, and through our comparison to other cell types we demonstrate the heightened sensitivity of developing oligodendrocytes to quaternary compound-induced cell death. We validated our *in vitro*

results *in vivo* through postnatal delivery of cetylpyridinium chloride to mouse pups. In this model, and in a 3-D model of human prenatal brain development, our data show that these chemicals are cytotoxic specifically to the oligodendrocyte lineage during critical periods for oligodendrocyte development. We report that quaternary compounds induce the integrated stress response in developing oligodendrocytes, resulting in CHOP accumulation and apoptosis which can be abrogated through combinatorial treatment with ISRIB and QVD-OPH. In genetic and inflammatory diseases, developing and regenerating oligodendrocytes are particularly sensitive to ER stress and subsequent prolonged activation of the integrated stress response in part due to the requirement of developing oligodendrocytes to produce large amounts of myelin proteins[46]. This sensitivity may underlie the specific toxicity of quaternary compounds and could initiate or exacerbate pathology in disease.

In developing oligodendrocytes, the IC_{50} values for quaternary compound toxicity are in the nanomolar range, similar to predicted blood concentrations for many quaternary ammonium compounds in children[47]. Both *in vitro* and *in vivo* we evaluated acute exposure to quaternary compounds, whereas chronic exposure spanning oligodendrocyte development could drive toxicity at even lower concentrations, given their capacity for bioaccumulation[45]. When considering cytotoxicity data in mouse and human oligodendrocytes and the potential risk for chronic exposure, our data demonstrating the ability of quaternary ammonium compounds to pass the blood brain barrier during the early postnatal period and the increased use of quaternary ammonium compounds raises significant health concerns for neurodevelopmental toxicity[48].

The pervasive use of organophosphate flame retardants has contaminated the environment and increased human exposure, demonstrated by the detection of these chemicals in human blood, urine, breast milk, and cerebrospinal fluid[49,50]. We show that the organophosphate flame retardant TDCIPP arrests the development of mouse oligodendrocytes both *in vitro* and *in vivo* and inhibits oligodendrocyte generation in human cortical organoids at concentrations similar to estimated blood concentrations in children[51]. Our results and the likelihood of organophosphate flame retardant exposure in children raise potential health concerns as these chemicals may reach higher concentrations in cerebrospinal fluid than blood[52].

Human epidemiological studies that evaluate prenatal exposure to TDCIPP have identified associations between maternal exposure and delayed cognitive development[33]. However, these studies focused on solely prenatal exposures. Therefore, the disruption of critical periods of oligodendrogenesis and myelination during neurodevelopment in infancy and childhood by organophosphate flame retardants has yet to be evaluated. We analyzed datasets from the US CDC's NHANES, spanning from 2013 to 2018, to identify associations between childhood exposure to organophosphate flame retardants and abnormal neurodevelopmental outcomes. Our logistic regression analyses demonstrate that there are significantly increased odds ratios for children with high urinary BDCIPP concentrations to report multiple abnormal cognitive and motor outcomes. Continued evaluation of organophosphate flame retardant exposure and direct measurements of white matter development in children would provide critical evidence that chemical-mediated perturbation of oligodendrocyte development influences abnormal cognitive and motor

outcomes. Although organophosphate flame retardants are pervasive and human exposure is ubiquitous, behavioral interventions are effective in reducing exposure to TDCIPP and could be considered to minimize potential risks to children[53].

This work reveals toxicological sensitivities in the oligodendrocyte lineage to common household chemicals and raises potential health concerns for exposure to these chemicals. Continued experimental and epidemiological studies are required to determine the full impact of exposure to quaternary ammonium and phosphonium compounds and organophosphate flame retardants. Results from this study will contribute to the scientific foundation that will inform decisions about regulatory or behavioral interventions designed to reduce chemical exposure and protect human health.

METHODS:

All methods comply with relevant ethical regulations including the International Society for Stem Cell Research 2021 Guidelines for Stem Cell Research and Clinical Translation, the National Institutes of Health Guidelines for the Care and Use of Laboratory Animals and the Case Western Reserve University Institutional Animal Care and Use Committee.

Induced pluripotent stem cell-derived OPC culture

Mouse OPCs were differentiated from mouse induced pluripotent stem cells (iPSCs) as previously described[21,54]. Briefly, iPSCs were removed from an irradiated mouse embryo fibroblast feeder layer with 1.5 mg/mL collagenase type IV (ThermoFisher, 17104019), dissociated with 0.25% trypsin-EDTA (ThermoFisher, 25200056), and seeded at $7.8x10^4$ cells/cm^2 on Costar Ultra-Low attachment plates (Sigma, CLS3471). Cells were cultured in media allowing for the expansion and maturation of OPCs for 9 days. On day 10, media was switched to OPC medium, comprised of N2B27 base medium, supplemented with 20 ng/mL FGF-2 (R&D Systems, 233-FB-010), and 20 ng/mL PDGF-AA (R&D Systems, 221-AA). N2B27 base medium consists of Dulbecco's Modified Eagle Medium/ Nutrient Mixture F-12 (DMEM/F-12; ThermoFisher 11320033), supplemented with 1X B-27 Supplement (ThemoFisher, 17504044), 1X N-2 MAX Supplement (ThermoFisher, 17502048), 1X GlutaMAX Supplement (ThermoFisher, 35050079). OPC medium was used over three passages to enrich for OPCs. OPC biological replicates were generated from independent mouse iPSC lines. Mouse iPSC-derived OPCs were used for all experiments unless otherwise noted.

Primary mouse OPC and astrocyte culture

All animal procedures were performed in accordance with the National Institutes of Health Guidelines for the Care and Use of Laboratory Animals and approved by the Case Western Reserve University Institutional Animal Care and Use Committee. Timed-pregnant mice (C57BL/6N) were ordered from Charles River (Wilmington, MA). Brains from both male and female mice were grossly dissected at postnatal day 2 (P2). Cortex tissue was isolated and dissociated using the Miltenyi Tumor Dissociation Kit (Miltenyi, 130-095-929) following the manufacturer's instructions. Following dissociation, cells were plated in poly-L-ornithine (Sigma, P3655) and laminin (Sigma, L2020) coated flasks

and cultured for 24 hours. Culture media consists of N2B27 base medium supplemented with 20 ng/mL FGF-2 (R&D Systems, 233-FB-010), and 50 units/mL-50ug/mL Penicillin-Streptomycin (ThermoFisher, 15070063). After 24 hours of culture, media was switched to astrocyte or OPC enrichment media. OPC enrichment media is comprised of N2B27 base media supplemented with 20 ng/mL PDGF-AA (R&D Systems, 221-AA), 10ng/mL NT-3 (R&D Systems 267-N3), 100 ng/mL IGF (R&D Systems, 291-GF-200), 10 μM cyclic AMP (Sigma, D0260), 100 ng/mL noggin (R&D Systems, 3344NG050) and 50 units/mL-50ug/mL Penicillin-Streptomycin (ThermoFisher, 15070063). OPCs were cultured in this media until the next passage, at which point 50 units/mL-50ug/mL Penicillin-Streptomycin was removed. Astrocyte enrichment media consists of 1:1 DMEM (ThermoFisher, 11960044)—Neurobasal Medium (ThermoFisher, 211-3-49), supplemented with 1X N-2 MAX Supplement (ThermoFisher, 17502048), 1X GlutaMAX Supplement (ThermoFisher, 35050079), 50 units/mL-50ug/mL Penicillin-Streptomycin (ThermoFisher, 15070063), 5 ug/mL N-acetyl cysteine (Sigma, A8199), 10 ng/mL CNTF (R&D 557-NT-010), 5 ng/mL HB-EGF (R&D Systems 259-HE-050), and 20 ng/mL FGF-2 (R&D Systems, 233-FB-010). Media changes were performed every 48 hours and cells were allowed to proliferate, grown to confluency, and either passaged once or cryopreserved. For terminal experiments, astrocytes were thawed and plated into 384-well plates (Perkin Elmer, 6057500) at a density of 4,000 cells per well. Cells were then cultured with maturation media, comprised of 1:1 DMEM and Neurobasal media, supplemented with 1X N-2 MAX, 5 ug/mL N-acetyl cysteine, 1X GlutaMAX Supplement, 1 mM Sodium Pyruvate (ThermoFisher, 11360-070), 5 ng/mL HB-EGF, 10 ng/mL CNTF, 50 ng/mL BMP4 (R&D, 314-BP-050) and 20 ng/mL FGF-2. After 48 hours of culture in astrocyte maturation media, cells were cultured in resting astrocyte media (1:1 DMEM/Neurobasal Medium supplemented with 5 ng/mL HB-EGF) for 72 hours.

Mouse fibroblast culture

Mouse embryonic fibroblasts (fibroblasts) were isolated as described previously[55]. Briefly, fibroblasts were collected from embryos at embryonic day 13.5 generated through mating BALB/c mice. Fibroblasts were expanded for one passage in media comprised of DMEM (11960-044) supplemented with 10% FBS, 1X MEM Non-Essential Amino Acids Solution (11140-050),1X GlutaMAX Supplement (ThermoFisher, 35050079), and 0.1mM 2-mercaptoethanol (M6250-250ML) and cryopreserved.

Mouse oligodendrocyte differentiation

OPCs were plated in 96-well plates (Fisher, 167008) coated with poly-L-ornithine (Sigma, P3655) and laminin (Sigma, L2020) at a seeding density of 40,000 cells per well, or 384-well plates coated with poly-D-lysine and laminin (Sigma, L2020) at a seeding density of 12,500 cells per well. Cells were plated in differentiation permissive media, comprised of N2B27 base medium, 10ng/mL NT-3 (R&D Systems 267-N3), 100 ng/mL IGF (R&D Systems, 291-GF-200), 10 μM cyclic AMP (Sigma, D0260), 100 ng/mL noggin (R&D Systems, 3344NG050), and 40 ng/mL T3 (Sigma, T6397) when noted. Cells were differentiated over 3 days and analyzed.

Immunocytochemistry

Live staining was performed for specific antigens (O1 and O4). Antibodies for O1 and O4 were diluted in N2B27 base medium supplemented with 5% Donkey Serum (v/v) (Jackson ImmunoResearch, 017-000-121) and added to wells for 18 minutes at 37°C. Cells were then fixed with 4% Paraformaldehyde (Electron Microscopy Sciences, HP1-100Kit) for 15 minutes at room temperature, washed with PBS, and incubated overnight at 4°C with primary antibody diluted in PBS supplemented with 5% Donkey Serum (v/v) and 0.1% Triton-X-100 (Sigma, T8787). Primary antibodies included anti-O1 (1:100, CCF Hybridoma core), anti-O4 (1:100, CCF Hybridoma core), and anti-MBP (1:4000, Abcam, ab7349). The following day cells were rinsed with PBS and incubated for 2 hours with the appropriate Alexa Fluor-conjugated secondary antibodies (2 μg/mL, Thermo Fisher, A21208 or A31571) and DAPI (1 μg/mL, Sigma, D8417).

Chemical screening

Chemicals from the US EPA Toxicity Forecaster (ToxCast) chemical library were obtained through a Material Transfer Agreement with the US EPA. This library contained 1,823 chemicals dissolved in dimethyl sulfoxide (DMSO) at a top target stock concentration of 20 mM (with some chemicals achieving lower stock concentrations based on solubility limits in DMSO) and was stored at −20°C. Screening of the chemical library on OPCs was performed as described previously[21]. CellCarrier Ultra 384-well plates (PerkinElmer, 6057500), pre-coated with poly-D-lysine, were coated with laminin (Sigma, L2020) diluted in N2B27 base media. Laminin was dispensed using an EL406 Microplate Washer Dispenser (BioTek) using a 5 μL dispense cassette (BioTek) and incubated for at least 1 hour at 37°C. OPCs were next dispensed in oligodendrocyte differentiation permissive media, at a density of 12,500 cells per well. OPCs were allowed to attach to the plates for 1 hour at 37°C and chemicals were added to plates at a 1:1000 dilution using a Janus automated workstation and 50 nL solid pin tool attachment. Each compound was added at a final test well concentration of 20 μM. Chemicals used for dose response validation were sourced from the primary screening library. DMSO (Sigma, D2650) was added at 1:1000 dilution to negative control wells and 40 ng/mL T3 (Sigma, T6397) was added to positive control wells. After 72 hours, cells were stained with anti-O1 (1:100, CCF Hybridoma core), fixed with 4% Paraformaldehyde (Electron Microscopy Sciences, HP1-100Kit), and imaged using the Operetta High Content Imaging and Analysis system (PerkinElmer).

Kinetics of oligodendrocyte differentiation

OPCs were seeded at a density of 40,000 cells per well in 96-well plates coated with poly-L-ornithine (Sigma, P3655) and laminin (Sigma, L2020) in differentiation permissive media supplemented with 40 ng/mL T3 (Sigma, T6397). Cells were treated with TDCIPP (Sigma, 32951), TMPP (Santa Cruz, sc-296611), or TBPP (Millipore, 34188) at a final concentration of 20uM. DMSO (Sigma, D2650), was added at 1:1000 to negative control wells. As described previously, cells were live stained with anti-O4 (1:100, CCF Hybridoma core), anti-O1 (1:100, CCF Hybridoma core), and fixed with 4% Paraformaldehyde (Electron Microscopy Sciences, HP1-100Kit) after 1, 2, and 3 days post-plating. Cells were then

stained overnight with anti-MBP (1:4000, Abcam, ab7349) followed by staining with DAPI (1 μg/mL, Sigma, D8417), and imaged.

High content imaging and quantification

The Operetta High Content Imaging and Analysis system was used to image all 96- and 384-well plates. For each well of the 96- and 384-well plates, 4 fields were captured at 20x magnification. The PerkinElmer Harmony and Columbus software was used to analyze images as described previously[22,56,57]. In brief, nuclei from live cells were identified by DAPI positivity, using thresholding to exclude cell debris or pyknotic nuclei. A region outside of each DAPI-positive nucleus, expanded by 50%, was used to identify oligodendrocytes by positive staining for oligodendrocyte markers (O1 in primary screen and O4, O1, or MBP in kinetics experiments) within this region. Expanded DAPI-positive nuclei that overlapped with O4, O1, or MBP staining were classified as oligodendrocytes. Cell viability was calculated by dividing the number of DAPI-positive nuclei in an experimental well by the average number of DAPI-positive cells in the negative control wells. Oligodendrocyte percentage was calculated by dividing the number of oligodendrocytes by DAPI-positive cells and normalized to negative control wells.

MTS assay

OPCs were seeded at a density of 12,500 cells per well in CellCarrier Ultra 384-well plates (PerkinElmer, 6057500), pre-coated with poly-D-lysine and laminin (Sigma, L2020) in differentiation permissive media. Cells were allowed to attach for 1 hour at 37°C and compounds were added to plates at a 1:1000 dilution at a final concentration of 20 μM using a Janus automated workstation. DMSO (Sigma, D2650) was added at 1:1000 dilution to negative control wells and 40 ng/mL T3 (Sigma, T6397) was added to positive control wells. Cell viability was assessed after 72 hours using a 3-(4,5-dimethylthiazol-2-yl)-5-(3-carboxymethoxyphenyl)-2-(4-sulfophenyl)-2H-tetrazolium (MTS) assay kit (Abcam, ab197010) according to the manufacturer's protocol. Absorbance at 490 nm was measured 4 hours after the addition of the MTS dye using a SynergyNEO2 plate reader (BioTek).

Quaternary compound dose response testing

The following quaternary compounds were independently sourced: methyltrioctylammonium chloride (Sigma, 69485), tributyltetradecylphosphonium chloride (AccuStandard, BIOC-105N), methylbenzethonium chloride (Sigma, M7379), dodecyltrimethylammonium chloride (Sigma, 44242), didecyldimethylammonium chloride (Sigma, 34466), C12-C14-alkyl(ethylbenzyl)dimethylammonium chloride (Sigma 32279), cetrimonium bromide (Selleck, S4242), cetylpyridinium chloride (Selleck, S4172), and benzalkonium chloride (Selleck, S5626). For dose response testing, OPCs were seeded in 96-well plates coated with poly-L-ornithine (Sigma, P3655) and laminin (Sigma, L2020) at a density of 40,000 cells per well, Astrocytes were thawed and seeded at a density of 17,000 cells per well and cultured as described previously for terminal experiments. Fibroblasts were seeded at a density of 17,000 cells per well in 96-well plates coated with 0.1% gelatin. Quaternary compounds were reconstituted using DMSO (Sigma D2650) and pinned to 96-well plates using a 96-well pin tool (V&P Scientific, VP409) 1 hour after cells were plated. After 72 hours, cells were fixed using 4% Paraformaldehyde (Electron Microscopy

Sciences, HP1-100Kit), and stained with DAPI (1 μg/mL, Sigma, D8417). DAPI-positive nuclei were imaged and quantified using the Operetta High Content Imaging and Analysis system (PerkinElmer) and Columbus software.

Human cortical organoid production

Human embryonic stem cell research was restricted to *in vitro* culture and *in vitro* cortical organoid generation using the human embryonic stem cell (hESC) line H7 (Wicell, WA07) and an in-house induced pluripotent stem cell line (hPSC) (CWRU22) derived from a healthy male. hESC and hPSC culture was performed following the International Society for Stem Cell Research 2021 Guidelines for Stem Cell Research and Clinical Translation. hESCs and hPSCs were expanded in mTesR1 media (Stem Cell Technologies, 85850) and cortical organoids were generated as previously described and with minor modifications[30]. Modifications include replacement of Y-27632 and dorsomorphin with CloneR (Stem Cell Technologies, 5889) and 150nM LDN193189 respectively during the first step in the generation of cortical organoids. For the first 6 days, organoids were cultured with media containing 10 μM SB-43152 (Sigma, S4317) and 150 nM LDN193189, followed by 20 ng/mL EGF (R&D Systems, 236-EG-200) and 20 ng/mL FGF-2 (R&D Systems, 233-FB-010) on days 7 to 25. On days 27 to 40 organoids were fed on alternate days with media containing 20 ng/mL NT-3 (R&D Systems, 267-N3) and 10 ng/mL BDNF (R&D Systems 248-BD). To expand OPC populations, 10 ng/mL PDGF-AA (R&D Systems, 221-AA) and 10 ng/mL IGF (R&D Systems, 291-GF-200) were added to organoid cultures every other day between days 51 and 60. To induce the differentiation of oligodendrocytes 40 ng/mL T3 (Sigma, T6397) was added on alternate days between days 60 to 70. Organoids were treated with DMSO or chemicals on alternating days beginning on day 60 and harvested on day 70. Methyltrioctylammonium chloride, cetylpyridinium chloride, C12-C14-Alkyl(ethylbenzyl)dimethylammonium chloride, and TDCIPP (Sigma, 32951) were added at their IC_{75} concentration.

Cortical organoid immunohistochemistry

Organoids were harvested on day 70, washed in PBS, and fixed overnight with ice-cold 4% Paraformaldehyde (Electron Microscopy Sciences, HP1-100Kit). On the following day organoids were washed with PBS and cryoprotected using a 30% sucrose solution. Organoids were then embedded in OCT (Electron Microscopy Sciences, 62550-12) and sectioned at 15 μm. Slides were washed with PBS and incubated overnight with anti-SOX10 (1:200, R&D, AF2864) anti-APC CC1 (1:200, Millipore, MABC200), anti-SOX2 (1:200, Thermo Fisher, MAB2018), and anti-NEUN (1:250, CST, 24307) followed by labeling with Alexa Fluor-conjugated secondary antibodies (2 μg/mL, Thermo Fisher). Slides were imaged at 20x magnification using a Hamamatsu Nanozoomer S60. Quantification of positive cells was performed using QuPath software (https://qupath.github.io/)[58].

Cell death inhibitor testing

OPCs were seeded in 384-well plates (PerkinElmer, 6057500) pre-coated with poly-D-lysine and laminin (Sigma, L2020) at a density of 12,500 cell per well and allowed to attach for 1 hour at 37°C. Cell death inhibitors quinoline-Val-Asp-Difluorophenoxymethylketone (QVD-OPH) (Selleck, S7311), ferrostatin-1 (Selleck, S7243), and necrostatin-1 (Selleck,

S8037) were added using a Janus automated workstation and 50 nL solid pin tool attachment in 8-point dose response (80 nM to 10 μM), and incubated for 1 hour at 37°C. Methyltrioctylammonium chloride, cetylpyridinium chloride, or C12-C14-Alkyl(ethylbenzyl) dimethylammonium chloride were added to all wells at IC_{50} concentrations, and oligodendrocytes were allowed to develop for 72 hours. Negative control wells contained only methyltrioctylammonium chloride or tributyltetradecylphosphonium chloride. Positive control wells contained vehicle (DMSO). Cells were fixed with 4% Paraformaldehyde (Electron Microscopy Sciences, HP1-100Kit) and stained with and DAPI (1 μg/mL, Sigma, D8417). Imaging was performed with the Operetta High Content Imaging and Analysis system (PerkinElmer) and the PerkinElmer Harmony and Columbus software was used to quantify DAPI-positive nuclei.

RNA sequencing

OPCs were seeded at a density of 100,000-150,000 cells/cm^2 in 6-well plates coated with poly-L-ornithine (Sigma, P3655) and laminin (Sigma, L2020) in differentiation permissive media and allowed to attach for one hour. OPCs were incubated with vehicle (DMSO), methyltrioctylammonium chloride, cetylpyridinium chloride or C12-C14-Alkyl(ethylbenzyl)dimethylammonium chloride at their IC_{75} concentrations for 4 hours. OPCs were then lysed in TRIzol (Invitrogen, 15596018) and RNA was extracted by phenol-chloroform extraction and purified using the RNeasy Mini Kit (Qiagen, 74104). Samples were sent to Novogene for library preparation and mRNA sequencing. Libraries were generated according to protocols from the NEBNext Poly(A) mRNA Magnetic Isolation Module (NEB, E7490L) and NEBNext Ultra RNA Library Prep Kit for Illumina (NEB, E7530L) and then evenly pooled and sequenced on the Illumina NovaSeq with 150bp paired-end reads and a read depth of at least 20 million reads per sample. Salmon 1.8.0. (https://github.com/COMBINE-lab/salmon)[59] was used to align reads to the mm10 genome and quantify transcript abundance as transcripts per million (TPM) values. The R package tximport was used to convert TPM values into gene-TPM abundance matrices. Differential gene expression analysis was performed using DESeq2 using genes considered expressed with TPM>1[60].

Gene set enrichment analysis

Gene set enrichment analysis (GSEA) software was used to calculated normalized enrichment scores, in hallmark datasets using 1000 gene-set permutations, weighted scoring, and signal-to-noise metrics (https://www.gsea-msigdb.org/gsea/index.jsp). GSEA was performed using ranked sets of differentially expressed genes (pval < 0.05). GSEA software generated normalized enrichment scores and false discovery rates. The integrated stress response gene set was curated from two published gene sets (Supplementary Table 3)[61,62].

qRT-PCR

OPCs were seeded at a density of 100,000-150,000 cells/cm^2 in poly-L-ornithine (Sigma, P3655) and laminin (Sigma, L2020) coated plates in differentiation permissive media. Fibroblasts were seeded at a density of 50,000-75,000 cells/cm^2 in plates coated with 0.1% gelatin (Sigma, G1890) in fibroblast media. Cells were allowed to attach for 1 hour prior

to quaternary compound addition. After 4 hours, cells were lysed using TRIzol (Invitrogen, 15596018) and RNA was isolated as described for RNA sequencing. RNA quantity and quality was assessed using a NanoDrop spectrophotometer and cDNA was synthesized using an iScript cDNA Synthesis Kit (Biorad, 1708891) following the manufacturer's instructions. qRT-PCR was performed using TaqMan gene expression assays (Thermo Fisher, 4444963) and run on an Applied Biosystems QuantStudio 3 real-time PCR system. *Rpl13a* (Mm05910660_g1) was used as an endogenous control and probes for *Ddit3* (Mm01135937_g1) were normalized to the endogenous control.

TDCIPP and quaternary compound postnatal administration and pharmacokinetics

All animal procedures were performed in accordance with the National Institutes of Health Guidelines for the Care and Use of Laboratory Animals and approved by the Case Western Reserve University Institutional Animal Care and Use Committee. Timed-pregnant C57BL/6N mice were purchased from Charles River (Wilmington, MA). All animals were housed in a temperature and humidity controlled environment, as well as a 12 h: 12h light:dark cycle. Mice had ad libitum access to rodent chow and water. To assess the ability of quaternary compounds to cross the blood brain barrier, on postnatal day 9, male and female mice were randomly assigned to treatment groups and administered water (vehicle), 10 mg/kg/day, or 100 mg/kg/day of one of three quaternary compounds. Compounds were delivered at a volume of 10 uL/gram body weight. On postnatal day 10, mice were gavaged and perfused with saline 90 minutes later to remove blood from the brain. Brain and liver tissue were dissected and snap frozen for pharmacokinetic analysis. For ten-day chemical exposure studies, on postnatal day 5, male and female mice were randomly assigned to control (vehicle) or one of two treated groups for each chemical. Control and experimental animals were co-housed with the dam. Treated groups were administered 10 mg/kg/day or 100 mg/kg/day TDCIPP in corn oil or 1 mg/kg/day or 10 mg/kg/day cetylpyridinium chloride in water. Controls were administered vehicle (corn oil or water). On postnatal day 14, mice were gavaged and perfused 90 minutes later with saline. Liver was dissected and snap frozen for pharmacokinetic analysis. Brain tissue was collected and cut in half. One half of each brain (sagittally-cut) was snap frozen for pharmacokinetic analysis and one half was fixed with 4% paraformaldehyde (Electron Microscopy Sciences, HP1-100Kit) for immunohistochemistry. Snap frozen brain tissue was homogenized in PBS. Homogenate from calibration standards and study samples were extracted through the addition of 4x volume of acetonitrile with 200 ng/mL internal standard using a Hamilton Nimbus liquid handler. Extracted samples were then analyzed by LC-MS-MS in the positive ion, turbo spray mode. The limit of quantification for quaternary compounds and TDCIPP was 1 ng/mL and 10 ng/mL respectively.

Immunohistochemistry

Sagittal-cut brains were fixed in paraformaldehyde overnight, washed with PBS and cryoprotected using a 30% sucrose solution. Brains were then embedded in OCT (Electron Microscopy Sciences, 62550-12) and sectioned at 15 μm. Slides were permeabilized for 30 minutes with 10% Triton-X-100 (Sigma, T8787), washed with PBS, and then incubated overnight with the following primary antibodies: anti-SOX10 (1:200, R&D, AF2864) anti-APC CC1 (1:200, Millipore, MABC200 or anti-NEUN (1:250, CST, 24307). Following

primary incubation, slides were washed and incubated with Alexa Fluor secondary antibodies (ThermoFisher). Slides were imaged using a Hamamatsu NanoZoomer S60 Digital slide scanner. Quantification of positive cells was performed using QuPath.

US EPA ToxCast data

Data from the US EPA ToxCast invitroDBv3.3, was used to assign use categories to chemical hits and obtain median cytotoxicity values. Chemical use categories were assigned based on "collected data on functional use" or "products use categories" obtained from the CompTox dashboard (https://comptox.epa.gov/dashboard/). Cytotoxicity median values were generated using data from the invitroDBv3.3 and the R package tcpl (ToxCast Analysis Pipeline)[63].

ToxPrint chemotype enrichment analysis

ToxPrint chemotype enrichment analysis to identify enriched ToxPrints was performed as previously described using the publicly available ToxPrint feature set (https://toxprint.org/) and Chemotyper visualization application (https://chemotyper.org/)[63]. In separate analyses, chemical sets of interest were assigned as the "positive" chemical set and the remaining chemicals were assigned as the "negative" chemical set. Fischer's exact test was used to calculate p values for enriched ToxPrints in the positive chemical set compared to the negative set. Odds ratios were calculated as described previously[64]. ToxPrints had a p value ≤ 0.05 and odds ratio ≥ 3 were considered significant and analyzed further.

Statistical analysis

GraphPad prism was used to perform curve-fitting for the calculation of IC_{50} and IC_{75} values and all statistical analyses unless otherwise specified. Data are typically presented as the mean ± standard deviation (SD) or standard error of the mean (SEM) as described in figure legends. A p value ≤ 0.05 was considered statistically significant. Non-linear regression was used for curve fitting when determining IC_{50} concentrations. For box-and-whisker plots, the box extends from 25^{th} to 75^{th} percentiles, with a line in the middle of the box at the median. Whiskers extend from the minimum to maximum values in the dataset. No statistical methods were used to pre-determine sample sizes but were determined by reference to previous publications. The Mann-Whitney U-test and Kruskal-Wallis tests were selected, as appropriate, when data distributions were determined to be non-normal by the Shapiro-Wilk test. In all other cases, data distributions were assumed to be normal but were not formally tested. Analysis of immunostaining was performed by blind investigators using QuPath or by automated scripts with the Perkin Elmer Columbus Image Analysis Software. Unless otherwise noted, biological replicates were generated from independent mPSC lines for all mPSC-derived oligodendrocyte experiments. For human organoid experiments, individual organoids generated from 4 independent batches were considered biological replicates.

NHANES data source and study population

Anonymized data from the National Health and Nutrition Examination Survey (NHANES) were downloaded from the US Centers for Disease Control and Prevention (CDC) website

(https://wwwn.cdc.gov/nchs/nhanes). The 2017-2018 NHANES was approved by the CDC's National Center for Health and Statistics Ethics Review Board (protocol #2018-01) and is provided as anonymized data for public download. NHANES data were downloaded from the, 2013-2014, 2015-2016, and 2017-2018 datasets and used for logistic regression analyses.

NHANES exposure assessment

Exposure to tris(1,3-dichloro-2-propyl) phosphate (TDCIPP) was assessed based on urinary concentrations of bis(1,3-dichloro-2-propyl) phosphate (BDCIPP). Levels of urine BDCIPP were measured in all children ages 3-5 years of age in the 2015-2016 and 2017-2018 datasets and a one-third subset of children ages 6-11 years of age in all data cycles. Detailed methods for the measurement of BDCIPP urine concentration are provided online via the NHANES website (https://wwwn.cdc.gov/nchs/nhanes). Briefly, BDCIPP concentration was determined by solid phase liquid extraction followed by isotope dilution-ultrahigh performance liquid chromatography-tandem mass spectrometry. The lower limit of detection (LLOD, in ng/mL) for this assay was 0.1. For analytes below the LLOD, an imputed fill value was generated by dividing the LLOD by the square root of 2.

NHANES outcomes

Two neurodevelopmental outcomes, including reported special education and gross motor impairment were assessed. A proxy provided answers to questions for children below age 16 years of age. Proxies were asked the following questions to assess motor dysfunction: "Does Sample Person (SP) have an impairment or health problem that limits his/her ability to walk/run/play?". Children over the age of 16 were asked "Do you have an impairment or health problem that limits your ability to walk/run?" For assessment of special education utilization children and proxies were asked "Does SP receive Special Education or Early Intervention Services?".

NHANES covariates

NHANES collects data on other covariates including demographic and socioeconomic information. Subject age was determined based on the participant's date of birth. Participant's gender was queried at the time of the survey. Race/ethnicity was divided into five categories: Mexican American, Other Hispanic, Non-Hispanic White, Non-Hispanic Black, Other Race-including multi-racial. Education level of the household reference person was split into two categories: less than college degree, and college graduate or above. Poverty income ratios were calculated by dividing family income to poverty guidelines determined by the Department of Health and Human Services for the given survey year. Ratios at or above 5.00 were coded as 5.0. Department of Health and Human Services poverty guidelines were utilized to determine the ratio of family income to poverty. Mother's age at birth was split into three categories: less than 25 years old, 25-35 years old, and greater than 35 years old. Prenatal smoke exposure was evaluated by yes/no answer to "Did (SP NAMES's) biological mother smoke at any time while she was pregnant with (him/her)?". Detailed information on all NHANES covariates is available online (https://wwwn.cdc.gov/nchs/nhanes).

NHANES analysis

Unweighted analyses were performed using GraphPad Prism. Density plots were generated in R using the R package “ggplot2”. All weighted analyses including proportion calculations and logistic regression were performed using R and environmental weight variables. NHANES data were imported using the R package “nhanesA” and analyzed using the R package “survey”. Logistic regression analyses specified strata, cluster, and environmental weight variables to account for the NHANES complex survey design. To assess the presence of non-linear relationships between urinary BDCIPP and neurodevelopmental outcomes, BDCIPP was evaluated in quartiles. We constructed the main model containing the following covariates: urinary creatinine, sex, age, race/ethnicity, ratio of family income to poverty, education level of the household reference person, mother’s age, and mother smoked while pregnant. Age, urinary creatinine, and ratio of family income to poverty were modeled as continuous variables while sex, race/ethnicity, education level of the household reference person, mother’s age, and mother smoked while pregnant were included as discrete covariates. Logistic regression analyses were visualized using the R package “gtsummary”.

DATA AVAILABILITY:

Primary screening results are available in Supplementary Table 1 and will be included in a future public release of the US EPA ToxCast database. RNA-seq datasets generated in this study have been deposited in Gene Expression Omnibus (https://www.ncbi.nlm.nih.gov/geo/) under accession code GSE244500. Data from the US CDC’s National Health and Nutrition Examination Survey utilized in this study is publicly available at https://wwwn.cdc.gov/Nchs/Nhanes/. The mm10 genome utilized in RNA sequencing analysis is publicly available from GENCODE.

CODE AVAILABILITY:

Epidemiological analyses were performed using publicly available packages and followed guidelines provided by NHANES.

Extended Data

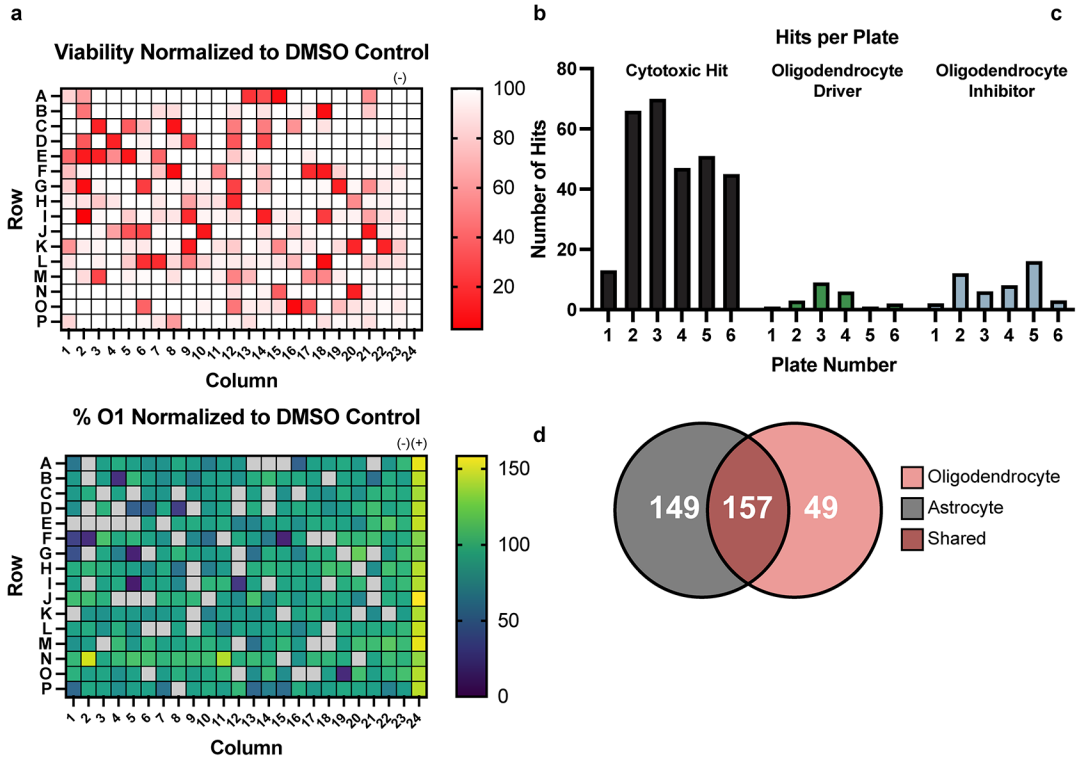

c

Use Category	Number of Chemicals
Biocide	91
Other, including pharmaceuticals	68
Dye	13
Antioxidant	8
Fragrance	6
Catalyst	4
Flame retardant	3
Plasticizer	2
UV stabilizer	2
Binder	1
Crosslinker	1
Flavorant	1
Heat stabilizer	1
Humectant	1
Preservative	1
Softener and conditioner	1
Stabilizing agent	1
Surfactant	1

Extended Data Fig. 1: Screening a library of environmental chemicals in developing oligodendrocytes identifies cytotoxic chemicals and modulators of oligodendrocyte generation.

a. Representative heatmaps of one of 6 primary screening 384-well plates depicting cytotoxic compounds (red), oligodendrocyte inhibitors (blue), and drivers (yellow). Viability and percent O1+ oligodendrocytes are normalized to DMSO vehicle control (−). Thyroid hormone, a known driver of oligodendrocyte generation, is included as a positive control (+) for oligodendrocyte development. Cytotoxic hits (gray) were omitted from heatmap displaying normalized O1 percentage. **b.** Quantification of hits across 6 primary screening plates showing distribution of chemicals identified as cytotoxic (black), drivers (green), and inhibitors (blue). **c.** Top use categories for 206 validated cytotoxic chemicals and the number of chemicals belonging to each category. **d.** Venn diagram showing the overlap of 206 validated cytotoxic chemicals identified in the oligodendrocyte screen compared to cytotoxic hits identified in an identical screen performed in mouse astrocytes.

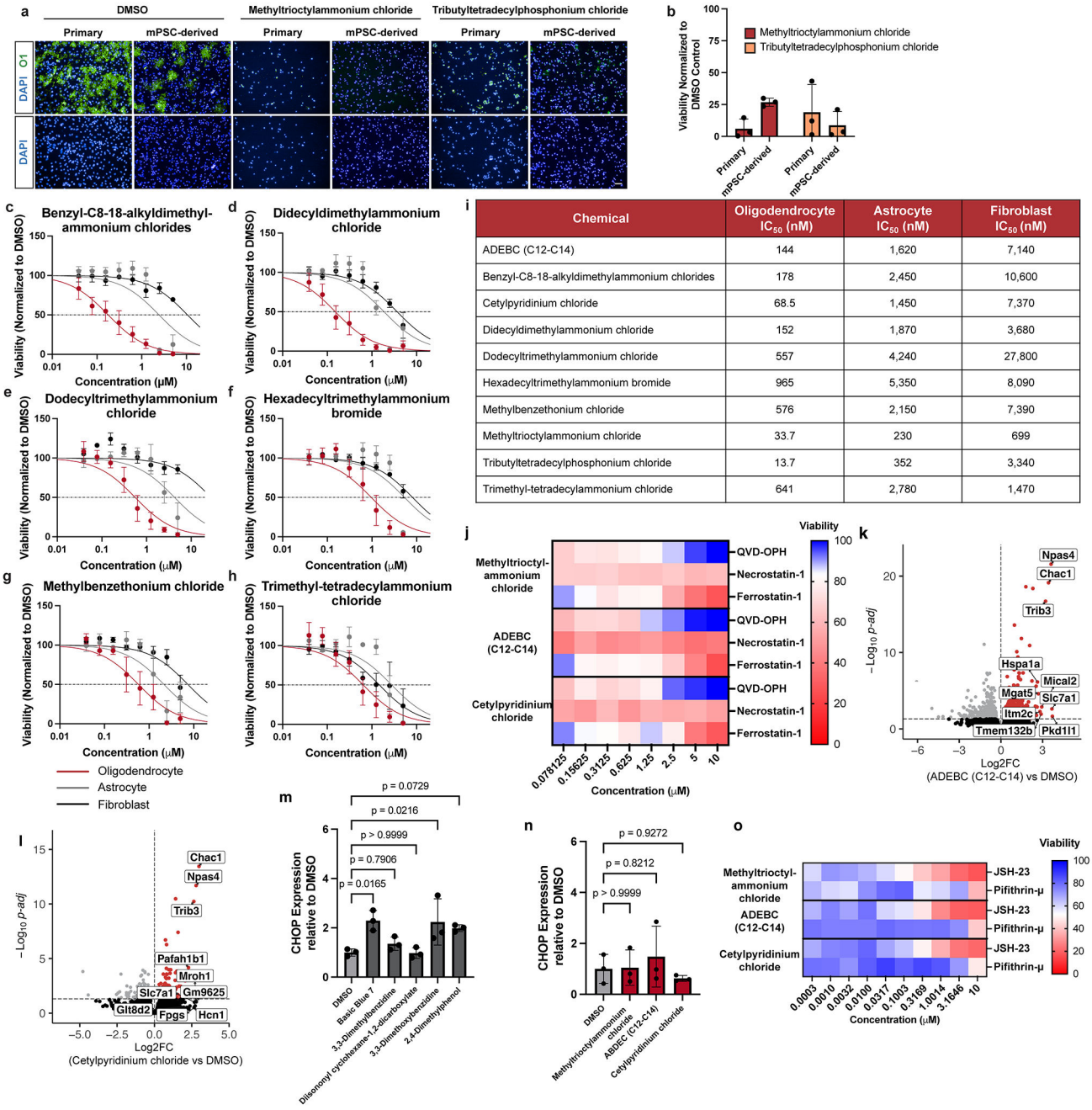

Chemical	Oligodendrocyte IC_{50} (nM)	Astrocyte IC_{50} (nM)	Fibroblast IC_{50} (nM)
ADEBC (C12-C14)	144	1,620	7,140
Benzyl-C8-18-alkyldimethylammonium chlorides	178	2,450	10,600
Cetylpyridinium chloride	68.5	1,450	7,370
Didecyldimethylammonium chloride	152	1,870	3,680
Dodecyltrimethylammonium chloride	557	4,240	27,800
Hexadecyltrimethylammonium bromide	965	5,350	8,090
Methylbenzethonium chloride	576	2,150	7,390
Methyltrioctylammonium chloride	33.7	230	699
Tributyltetradecylphosphonium chloride	13.7	352	3,340
Trimethyl-tetradecylammonium chloride	641	2,780	1,470

Extended Data Fig. 2: Quaternary compounds are selectively cytotoxic to oligodendrocytes through activation of the integrated stress response.

a-b. mPSC-derived oligodendrocytes and primary mouse oligodendrocytes were treated with 20 μM methyltrioctylammonium chloride and tributyltetradecylphosphonium chloride. **a**. Representative images showing DAPI and O1 immunostaining. Scale bar, 50 μm. **b**. Quantification of viability normalized to DMSO. Data are mean ± SD, n=3 biological replicates. **c-h.** Viability of mouse PSC-derived oligodendrocytes, primary astrocytes, and fibroblasts, normalized to DMSO after treatment with quaternary compounds. Data are

mean ± SEM, n=3 biological replicates. **i.** IC_{50} concentrations of quaternary compounds in mouse oligodendrocytes, astrocytes, and fibroblasts, n=3 biological replicates. **j.** Viability of oligodendrocytes normalized to DMSO cultured in the presence of methyltrioctylammonium chloride, ADEBC (C12-C14), or cetylpyridinium chloride at their respective IC_{75} and QVD-OPH, necrostatin-1, and ferrostatin-1. Data are mean, n=3 biological replicates **k,l.** Volcano plot of differentially expressed genes in oligodendrocytes treated with 370 nM (IC_{75}) ADEBC (C12-C14) (**k**) or 181 nM (IC_{75}) cetylpyridinium chloride (**l**) for 4 hours. Log2FC and padj were calculated with DESeq2. Genes highlighted in red increased (padj ≤ 0.05), n=3 biological replicates. Top 10 genes with the greatest Log2FC are labelled. **m.** qRT-PCR of CHOP in oligodendrocytes treated with DMSO, or top toxic compounds identified in the primary screen (not quaternary compounds). Oligodendrocytes were cultured for 4 hours in the presence of chemicals at IC_{75} or 20 μM if the calculated IC_{75} exceeded the primary screening concentration (388 nM Basic Blue 7, 20 μM 3,3'-dimethylbenzidine, 7.14 μM diisononyl cyclohexane-1,2-dicarboxylate, 1.82 μM 3,3'-dimethoxybenzidine, or 20 μM 2,4-dimethylphenol). Data are mean ± SD, n=3 biological replicates. p-values calculated using one-way ANOVA with Dunnett post-test correction for multiple comparisons. **n.** qRT-PCR of CHOP in fibroblasts treated for 4 hours normalized to DMSO. Quaternary compounds were tested at their IC_{75} (calculated from dose response testing in fibroblasts) or 20 μM if IC_{75} > 20 μM (2.0 μM methyltrioctylammonium chloride, 18.8 μM ADEBC (C12-C14), 20 μM cetylpyridinium chloride). Data are mean ± SD, n=3 biological replicates. p-values calculated using one-way ANOVA with Dunnett post-test correction for multiple comparisons. **o.** Oligodendrocyte viability (normalized to DMSO) after treatment with quaternary compounds (IC_{75}) and JSH-23 or Pifithrin-μ. Data shown as mean, n=3 biological replicates.

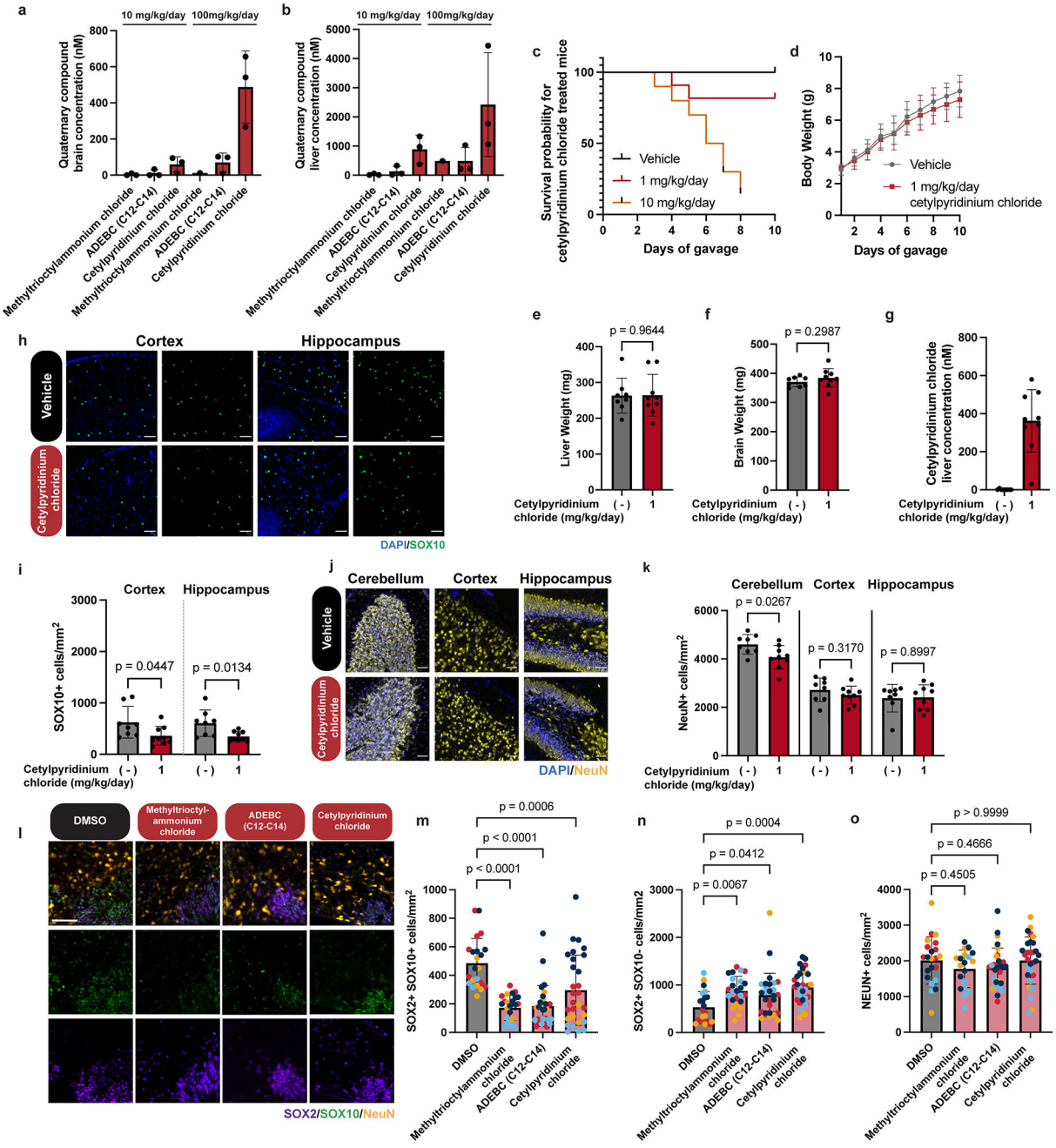

Extended Data Fig. 3: Quaternary compounds are toxic to mouse oligodendrocytes *in vivo* and in human cortical organoids.

a,b. Brain and liver concentration of methyltrioctylammonium chloride, ADEBC (C12-C14), and cetylpyridinium chloride after oral gavage (P9-P10). Data are mean ± SD, n=3 or 1 mice (100 mg/kg/day methyltrioctylammonium chloride mice presented from n=1 mouse due to lethality to other mice included in the study). **c.** Survival of mice treated with vehicle or cetylpyridinium chloride, n=8 (vehicle), n=10 (10 mg/kg/day), n=11 (1 mg/kg/day). Mice were considered dead if found dead in their cage or cannibalized by

dam. **d-k.** Mice were gavaged P5-P14 with vehicle (water) or 1 mg/kg/day cetylpyridinium chloride. Measurement of daily body (**d**), P14 liver (**e**), and P14 brain (**f**) weights. **g**. P14 cetylpyridinium chloride liver concentration, with analyte concentrations below the lower limit of detection (1 ng/mL) coded as 0. **h**. Representative images showing DAPI and SOX10 immunostaining. **i**. Quantification of oligodendrocyte lineage cell density (SOX10+ per mm^2) in cortex and hippocampus of P14 mice. **j**. Representative images showing DAPI and NEUN immunostaining. **k**. Quantification of neuron density (NEUN+ per mm^2) in cerebellum, cortex, and hippocampus of P14 mice. Data are mean ± SD, n=8 or 9 mice. p-values calculated using unpaired two-tailed t test (**e, f, i, k**). Scale bars, 50 μm (**h, j**). **l-o.** Human cortical organoids were treated with DMSO, 94 nM methyltrioctylammonium chloride, 370 nM ADEBC (C12-C14), or 181 nM cetylpyridinium chloride (IC_{75}). **l**. Representative images showing immunostaining of oligodendrocyte lineage cells (SOX10+), progenitors (SOX2+), and neurons (NeuN+). Scale bar, 50 μm. Quantification of pre-OPC (SOX2+SOX10+ per mm^2) (**m**), other progenitor (SOX2+SOX10− per mm^2) (**n**), and neuron (NeuN+ per mm^2) (**o**) densities in whole cortical organoids. Data are mean ± SD, n= 22, 24, 29, or 30 biological replicates (individual organoids from 4 independent batches), colored based on batch. p-values calculated using one-way ANOVA with Dunnett post-test correction for multiple comparisons.

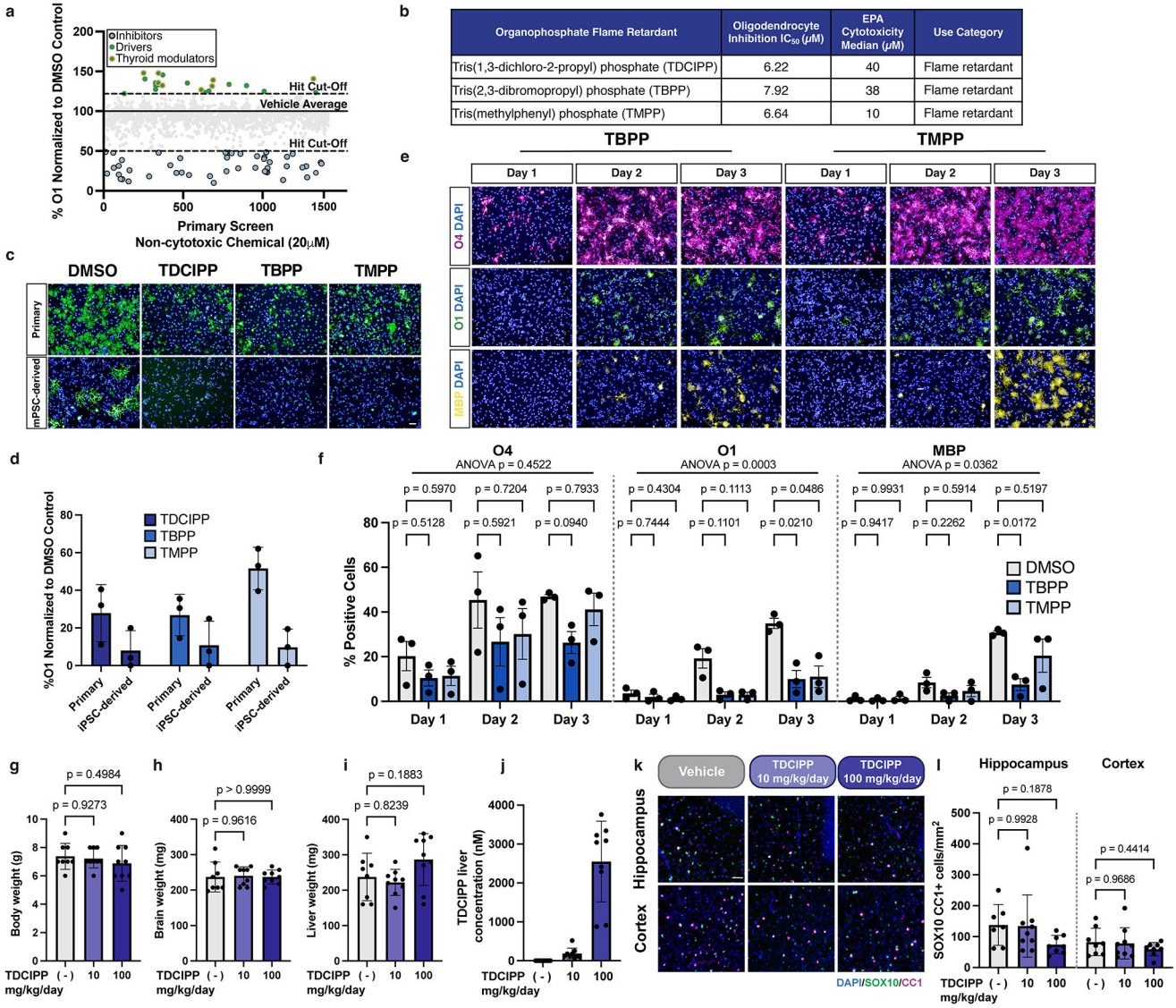

Organophosphate Flame Retardant	Oligodendrocyte Inhibition IC_{50} (μM)	EPA Cytotoxicity Median (μM)	Use Category
Tris(1,3-dichloro-2-propyl) phosphate (TDCIPP)	6.22	40	Flame retardant
Tris(2,3-dibromopropyl) phosphate (TBPP)	7.92	38	Flame retardant
Tris(methylphenyl) phosphate (TMPP)	6.64	10	Flame retardant

Extended Data Fig. 4. Organophosphate flame retardants inhibit the development of mouse oligodendrocytes *in vitro* and *in vivo*.

a. Primary chemical screen of 1,531 non-cytotoxic environmental chemicals showing the effect of individual chemicals on oligodendrocyte generation, presented as percent O1+ cells normalized to the DMSO control, as shown in Fig. 2a. Dotted lines show the hit cutoffs for drivers and inhibitors. Drivers increase O1+ percentage by 22% (>3 SDs). Inhibitors reduce O1+ percentage by more than 50% (>7 SDs). Thyroid modulators are highlighted in yellow. **b.** IC_{50} concentrations, cytotoxicity median values, and use categories for three organophosphate esters identified as inhibitors of oligodendrocyte development, n=3 biological replicates. **c-d.** mPSC-derived OPCs and mouse primary OPCs were treated with organophosphate flame retardants (20 μM). **c**. Representative images showing DAPI and O1 immunostaining, scale bar, 50 μm. **d**. Quantification of oligodendrocytes (O1+). **e-f.** mPSC-derived OPCs were treated with 20 μM TBPP or TMPP. Representative images (**e**) and quantification (**f**) of early (O4+), intermediate (O1+), and late (MBP+)

oligodendrocytes. Control images and TDCIPP treated oligodendrocytes are shown in Fig. 2e. Nuclei are marked with DAPI. Scale bar, 50 μm (**e**). Data are mean ± SEM, n=3 biological replicates p-values calculated using two-way ANOVA (ANOVA p=) for overall chemical differences with Dunnett's multiple comparison test for differences within each time point (p =) (**f**). **g-l.** Mice were treated with vehicle (corn oil), 10 mg/kg/day, or 100 mg/kg/day TDCIPP. Measurement of P14 body (**g**), brain (**h**), and liver (**i**) weights. **j**. TDCIPP liver concentrations at P14, with analyte concentrations below lower limit of detection (10 ng/mL) coded as 0. **k**. Representative images showing DAPI, SOX10, and CC1 immunostaining Scale bar, 50 μm. **l**. Quantification of oligodendrocyte density (SOX10+CC1+ per mm^2) in the hippocampus and cortex of P14 mice. Data are mean ± SD from n = 8 or 9 mice (**g-j, l**). p-values were calculated using one-way ANOVA with Dunnett post-test correction for multiple comparisons (**g-i, l**).

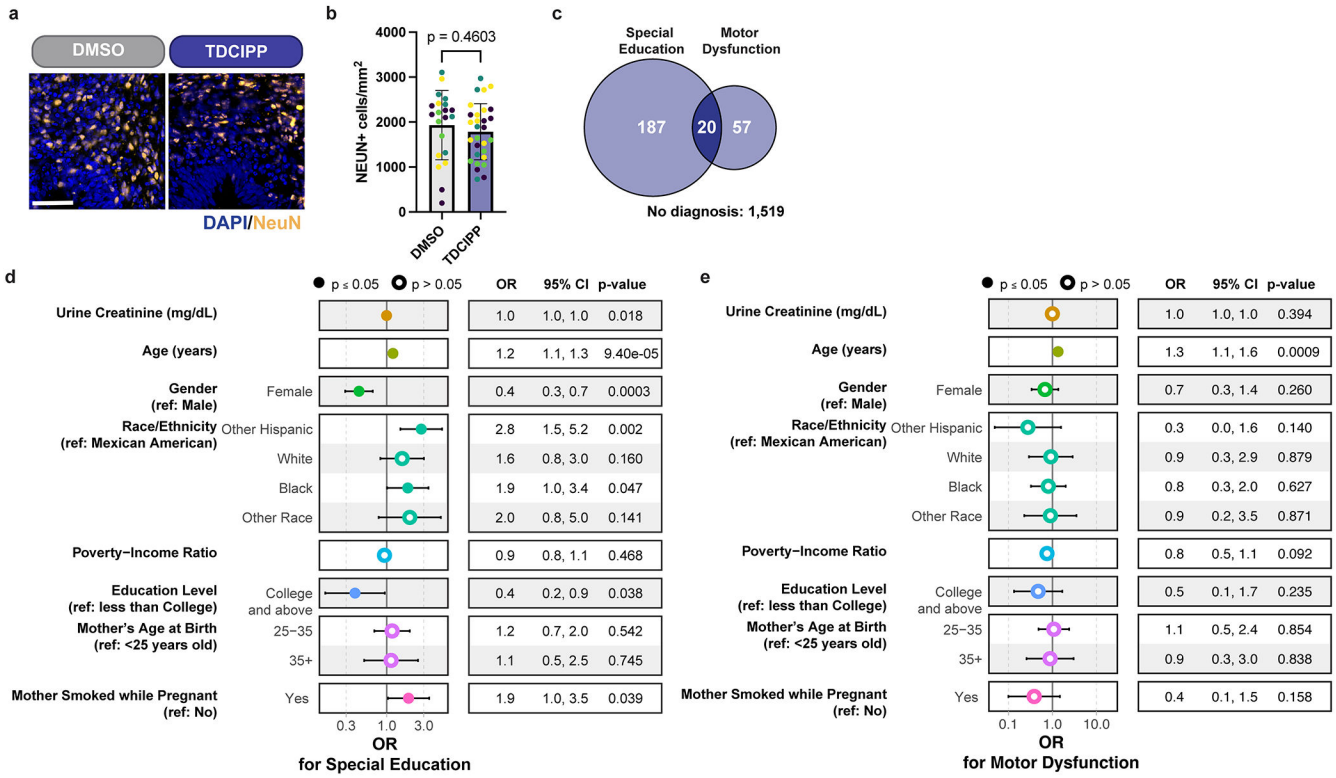

Extended Data Fig. 5: TDCIPP is associated with abnormal neurodevelopmental outcomes in children.

a. Representative images of human cortical organoids treated with 18.7 μM TDCIPP for 10 days, showing DAPI and NEUN immunostaining. Scale bar, 50 μm. **b.** Quantification of neurons (NEUM+ per mm^2) in whole cortical organoids. Data are mean ± SD from n = 21 or 29 biological replicates (individual organoids from 4 independent batches). Data points are colored based on organoid batch. p-values calculated using unpaired two-tailed t test. **c.** Venn diagram showing co-occurrence of two neurodevelopmental outcomes in the study population. **d-e.** Adjusted odds ratio and associated p-values for covariates used in the logistic regression model for the neurodevelopmental outcomes requiring special education and gross motor dysfunction, n = 1564 or 1566. Significant odds ratios (p-value ≤ 0.05) are

indicated by closed circles. Closed or open circles are the odds ratio and error bars indicate the 95% CI. Odds ratios and p-values were generated and visualized with the “survey” and “gtsummary” R packages. The Wald test was used to calculate p-values.

Supplementary Material

Refer to Web version on PubMed Central for supplementary material.

ACKNOWLEDGEMENTS:

This work was supported by grants from the National Institutes of Health R35NS116842 (P.J.T.), F31NS124282 (E.F.C.), T32NS077888 (E.F.C.), and T32GM007250 (E.F.C.). B.L.L.C. is supported by a NMSS Career Transition Fellowship. M.A.S. is supported by Howard Hughes Medical Institute Hanna H. Gray Fellowship and The New York Stem Cell Foundation Druckenmiller Fellowship. Institutional support was provided by CWRU School of Medicine and philanthropic support was generously contributed by sTF5 Care, and the, Long, Walter, Peterson, Goodman, and Geller families. The funders had no role in study design, data collection and analysis, decision to publish or preparation of the manuscript. Additional support was provided by the Small Molecule Drug Development and Light Microscopy Imaging core facilities of the CWRU Comprehensive Cancer Center (P30CA043703). The US Environmental Protection Agency provided the ToxCast screening library through MTA with CWRU and supported the effort of EPA employees (T.J.S. and K.P-F.). We are grateful to D. Adams, A. Wynshaw-Boris, D. Kassel, K. Carr, J. Kristell, K. Allan, E. Shick, R. Ziar, A. Sterling, and A. Gartley for technical assistance and/or discussion and C. Lilliehook for editorial support.

DISCLAIMER

This work was supported in part by the US Environmental Protection Agency and has been reviewed and approved for publication by the US EPA’s Center for Computational Toxicology and Exposure. Approval for publication does not signify that the contents reflect the views of the Agency, nor does mention of trade names or commercial products constitute an endorsement or recommendation for use.

REFERENCES:

1. Sanmarco LM, et al. Identification of environmental factors that promote intestinal inflammation. Nature (2022).
2. Wheeler MA, et al. Environmental Control of Astrocyte Pathogenic Activities in CNS Inflammation. Cell 176, 581–596 e518 (2019). [PubMed: 30661753]
3. Lidsky TI & Schneider JS Lead neurotoxicity in children: basic mechanisms and clinical correlates. Brain 126, 5–19 (2003). [PubMed: 12477693]
4. Grandjean P & Landrigan PJ Neurobehavioural effects of developmental toxicity. Lancet Neurol 13, 330–338 (2014). [PubMed: 24556010]
5. Grandjean P & Landrigan PJ Developmental neurotoxicity of industrial chemicals. Lancet 368, 2167–2178 (2006). [PubMed: 17174709]
6. Landrigan PJ, et al. Neuropsychological dysfunction in children with chronic low-level lead absorption. Lancet 1, 708–712 (1975). [PubMed: 47481]
7. Jacobson JL & Jacobson SW Intellectual impairment in children exposed to polychlorinated biphenyls in utero. N Engl J Med 335, 783–789 (1996). [PubMed: 8703183]
8. Li Q, et al. Prevalence of Autism Spectrum Disorder Among Children and Adolescents in the United States From 2019 to 2020. JAMA Pediatr 176, 943–945 (2022). [PubMed: 35789247]
9. Chung W, et al. Trends in the Prevalence and Incidence of Attention-Deficit/Hyperactivity Disorder Among Adults and Children of Different Racial and Ethnic Groups. JAMA Netw Open 2, e1914344 (2019). [PubMed: 31675080]
10. Zhou T, et al. A hPSC-based platform to discover gene-environment interactions that impact human beta-cell and dopamine neuron survival. Nat Commun 9, 4815 (2018). [PubMed: 30446643]
11. Caporale N, et al. From cohorts to molecules: Adverse impacts of endocrine disrupting mixtures. Science 375, eabe8244 (2022). [PubMed: 35175820]

12. Bercury KK & Macklin WB Dynamics and mechanisms of CNS myelination. Dev Cell 32, 447–458 (2015). [PubMed: 25710531]
13. Nave KA Myelination and the trophic support of long axons. Nat Rev Neurosci 11, 275–283 (2010). [PubMed: 20216548]
14. Elitt MS, et al. Suppression of proteolipid protein rescues Pelizaeus-Merzbacher disease. Nature 585, 397–403 (2020). [PubMed: 32610343]
15. Chang A, Tourtellotte WW, Rudick R & Trapp BD Premyelinating oligodendrocytes in chronic lesions of multiple sclerosis. N Engl J Med 346, 165–173 (2002). [PubMed: 11796850]
16. Jakel S, et al. Altered human oligodendrocyte heterogeneity in multiple sclerosis. Nature 566, 543–547 (2019). [PubMed: 30747918]
17. Silbereis JC, Pochareddy S, Zhu Y, Li M & Sestan N The Cellular and Molecular Landscapes of the Developing Human Central Nervous System. Neuron 89, 248–268 (2016). [PubMed: 26796689]
18. Giedd JN, et al. Brain development during childhood and adolescence: a longitudinal MRI study. Nat Neurosci 2, 861–863 (1999). [PubMed: 10491603]
19. Breinlinger S, et al. Hunting the eagle killer: A cyanobacterial neurotoxin causes vacuolar myelinopathy. Science 371(2021).
20. Klose J, et al. Neurodevelopmental toxicity assessment of flame retardants using a human DNT in vitro testing battery. Cell Biol Toxicol 38, 781–807 (2022). [PubMed: 33969458]
21. Lager AM, et al. Rapid functional genetics of the oligodendrocyte lineage using pluripotent stem cells. Nat Commun 9, 3708 (2018). [PubMed: 30213958]
22. Najm FJ, et al. Drug-based modulation of endogenous stem cells promotes functional remyelination in vivo. Nature 522, 216–220 (2015). [PubMed: 25896324]
23. Najm FJ, et al. Rapid and robust generation of functional oligodendrocyte progenitor cells from epiblast stem cells. Nat Methods 8, 957–962 (2011). [PubMed: 21946668]
24. Richard AM, et al. ToxCast Chemical Landscape: Paving the Road to 21st Century Toxicology. Chem Res Toxicol 29, 1225–1251 (2016). [PubMed: 27367298]
25. Sommers KJ, et al. Quaternary Phosphonium Compounds: An Examination of Non-Nitrogenous Cationic Amphiphiles That Evade Disinfectant Resistance. ACS Infect Dis 8, 387–397 (2022). [PubMed: 35077149]
26. Hora PI, Pati SG, McNamara PJ & Arnold WA Increased Use of Quaternary Ammonium Compounds during the SARS-CoV-2 Pandemic and Beyond: Consideration of Environmental Implications. Environ Sci Tech Let 7, 622–631 (2020).
27. Takeda R, et al. Antiviral effect of cetylpyridinium chloride in mouthwash on SARS-CoV-2. Sci Rep 12, 14050 (2022). [PubMed: 35982118]
28. Xiao S, Yuan Z & Huang Y Disinfectants against SARS-CoV-2: A Review. Viruses 14(2022).
29. Costa-Mattioli M & Walter P The integrated stress response: From mechanism to disease. Science 368(2020).
30. Madhavan M, et al. Induction of myelinating oligodendrocytes in human cortical spheroids. Nat Methods 15, 700–706 (2018). [PubMed: 30046099]
31. Paşca SP, et al. A nomenclature consensus for nervous system organoids and assembloids. Nature 609, 907–910 (2022). [PubMed: 36171373]
32. Paul-Friedman K, et al. Limited Chemical Structural Diversity Found to Modulate Thyroid Hormone Receptor in the Tox21 Chemical Library. Environ Health Perspect 127, 97009 (2019). [PubMed: 31566444]
33. Liu W, et al. Prenatal exposure to halogenated, aryl, and alkyl organophosphate esters and child neurodevelopment at two years of age. J Hazard Mater 408, 124856 (2021). [PubMed: 33383451]
34. Hoffman K, Gearhart-Serna L, Lorber M, Webster TF & Stapleton HM Estimated tris(1,3-dichloro-2-propyl) phosphate exposure levels for US infants suggest potential health risks. Environ Sci Technol Lett 4, 334–338 (2017). [PubMed: 34853794]
35. Ciesielski T, et al. Cadmium exposure and neurodevelopmental outcomes in U.S. children. Environ Health Perspect 120, 758–763 (2012). [PubMed: 22289429]

36. Kwon S & O'Neill M Socioeconomic and Familial Factors Associated with Gross Motor Skills among US Children Aged 3-5 Years: The 2012 NHANES National Youth Fitness Survey. Int J Environ Res Public Health 17(2020).
37. Steadman PE, et al. Disruption of Oligodendrogenesis Impairs Memory Consolidation in Adult Mice. Neuron 105, 150–164 e156 (2020). [PubMed: 31753579]
38. McKenzie IA, et al. Motor skill learning requires active central myelination. Science 346, 318–322 (2014). [PubMed: 25324381]
39. Xiao L, et al. Rapid production of new oligodendrocytes is required in the earliest stages of motor-skill learning. Nat Neurosci 19, 1210–1217 (2016). [PubMed: 27455109]
40. Kleinstreuer NC, et al. Phenotypic screening of the ToxCast chemical library to classify toxic and therapeutic mechanisms. Nat Biotechnol 32, 583–591 (2014). [PubMed: 24837663]
41. Hogberg HT, et al. Organophosphorus flame retardants are developmental neurotoxicants in a rat primary brainsphere in vitro model. Arch Toxicol 95, 207–228 (2021). [PubMed: 33078273]
42. Renner H, et al. Cell-Type-Specific High Throughput Toxicity Testing in Human Midbrain Organoids. Front Mol Neurosci 14, 715054 (2021). [PubMed: 34335182]
43. Chesnut M, Hartung T, Hogberg H & Pamies D Human Oligodendrocytes and Myelin In Vitro to Evaluate Developmental Neurotoxicity. Int J Mol Sci 22(2021).
44. United States Environmental Protection Agency: Disinfectants for Coronavirus (COVID-19); https://www.epa.gov/coronavirus/about-list-n-disinfectants-coronavirus-covid-19-0.
45. Zheng G, Webster TF & Salamova A Quaternary Ammonium Compounds: Bioaccumulation Potentials in Humans and Levels in Blood before and during the Covid-19 Pandemic. Environ Sci Technol 55, 14689–14698 (2021). [PubMed: 34662096]
46. Lin W & Popko B Endoplasmic reticulum stress in disorders of myelinating cells. Nat Neurosci 12, 379–385 (2009). [PubMed: 19287390]
47. Li D, Sangion A & Li L Evaluating consumer exposure to disinfecting chemicals against coronavirus disease 2019 (COVID-19) and associated health risks. Environ Int 145, 106108 (2020). [PubMed: 32927283]
48. Herron JM, et al. Multiomics Investigation Reveals Benzalkonium Chloride Disinfectants Alter Sterol and Lipid Homeostasis in the Mouse Neonatal Brain. Toxicological Sciences 171, 32–45 (2019). [PubMed: 31199489]
49. Patisaul HB, et al. Beyond Cholinesterase Inhibition: Developmental Neurotoxicity of Organophosphate Ester Flame Retardants and Plasticizers. Environ Health Perspect 129, 105001 (2021). [PubMed: 34612677]
50. Hou M, Zhang B, Fu S, Cai Y & Shi Y Penetration of Organophosphate Triesters and Diesters across the Blood-Cerebrospinal Fluid Barrier: Efficiencies, Impact Factors, and Mechanisms. Environ Sci Technol 56, 8221–8230 (2022). [PubMed: 35658413]
51. Blum A, et al. Organophosphate Ester Flame Retardants: Are They a Regrettable Substitution for Polybrominated Diphenyl Ethers? Environ Sci Technol Lett 6, 638–649 (2019). [PubMed: 32494578]
52. Hou M, Zhang B, Fu S, Cai Y & Shi Y Penetration of Organophosphate Triesters and Diesters across the Blood–Cerebrospinal Fluid Barrier: Efficiencies, Impact Factors, and Mechanisms. Environmental Science & Technology 56, 8221–8230 (2022).
53. Gibson EA, et al. Flame retardant exposure assessment: findings from a behavioral intervention study. J Expo Sci Environ Epidemiol 29, 33–48 (2019). [PubMed: 29950671]

METHODS-ONLY REFERENCES:

54. Najm FJ, et al. Isolation of epiblast stem cells from preimplantation mouse embryos. Cell Stem Cell 8, 318–325 (2011). [PubMed: 21362571]
55. Najm FJ, et al. Transcription factor-mediated reprogramming of fibroblasts to expandable, myelinogenic oligodendrocyte progenitor cells. Nat Biotechnol 31, 426–433 (2013). [PubMed: 23584611]
56. Allan KC, et al. Non-canonical Targets of HIF1a Impair Oligodendrocyte Progenitor Cell Function. Cell Stem Cell 28, 257–272 e211 (2021). [PubMed: 33091368]

57. Hubler Z, et al. Accumulation of 8,9-unsaturated sterols drives oligodendrocyte formation and remyelination. Nature 560, 372–376 (2018). [PubMed: 30046109]

58. Bankhead P, et al. QuPath: Open source software for digital pathology image analysis. Sci Rep 7, 16878 (2017). [PubMed: 29203879]

59. Patro R, Duggal G, Love MI, Irizarry RA & Kingsford C Salmon provides fast and bias-aware quantification of transcript expression. Nat Methods 14, 417–419 (2017). [PubMed: 28263959]

60. Love MI, Huber W & Anders S Moderated estimation of fold change and dispersion for RNA-seq data with DESeq2. Genome Biol 15, 550 (2014). [PubMed: 25516281]

61. Adamson B, et al. A Multiplexed Single-Cell CRISPR Screening Platform Enables Systematic Dissection of the Unfolded Protein Response. Cell 167, 1867–1882 e1821 (2016). [PubMed: 27984733]

62. Wong YL, et al. eIF2B activator prevents neurological defects caused by a chronic integrated stress response. Elife 8(2019).

63. Judson R, et al. Analysis of the Effects of Cell Stress and Cytotoxicity on In Vitro Assay Activity Across a Diverse Chemical and Assay Space. Toxicol Sci 153, 409 (2016). [PubMed: 27605417]

64. Paul Friedman K, et al. Utility of In Vitro Bioactivity as a Lower Bound Estimate of In Vivo Adverse Effect Levels and in Risk-Based Prioritization. Toxicol Sci 173, 202–225 (2020). [PubMed: 31532525]

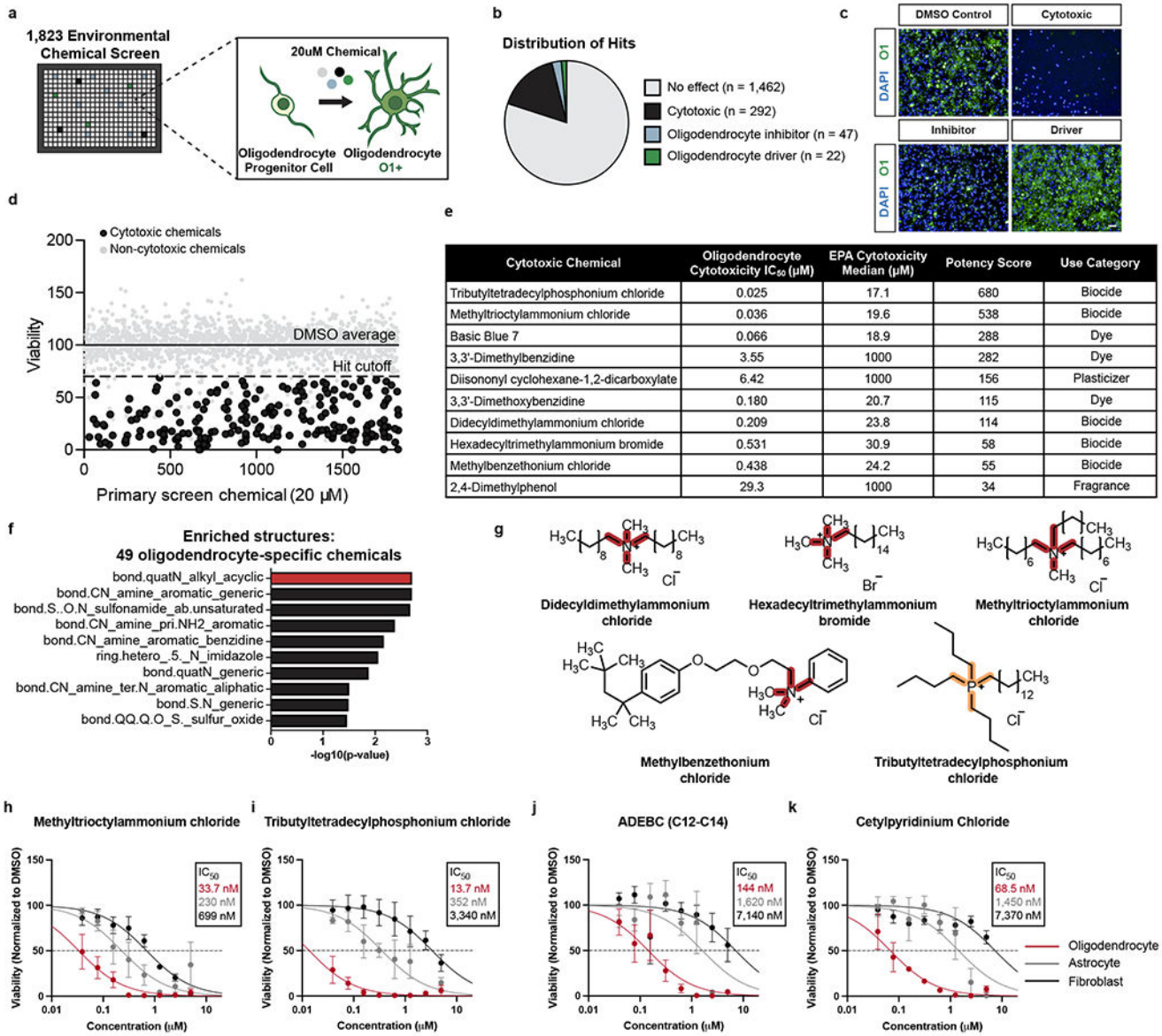

Cytotoxic Chemical	Oligodendrocyte Cytotoxicity IC_{50} (μM)	EPA Cytotoxicity Median (μM)	Potency Score	Use Category
Tributyltetradecylphosphonium chloride	0.025	17.1	680	Biocide
Methyltrioctylammonium chloride	0.036	19.6	538	Biocide
Basic Blue 7	0.066	18.9	288	Dye
3,3'-Dimethylbenzidine	3.55	1000	282	Dye
Diisononyl cyclohexane-1,2-dicarboxylate	6.42	1000	156	Plasticizer
3,3'-Dimethoxybenzidine	0.180	20.7	115	Dye
Didecyldimethylammonium chloride	0.209	23.8	114	Biocide
Hexadecyltrimethylammonium bromide	0.531	30.9	58	Biocide
Methylbenzethonium chloride	0.438	24.2	55	Biocide
2,4-Dimethylphenol	29.3	1000	34	Fragrance

Fig. 1: Quaternary compounds are potently cytotoxic to developing oligodendrocytes.

a. Schematic of the primary chemical screen in mPSC-derived oligodendrocytes. **b.** Pie chart of chemical hit categories from the primary screen. **c.** Representative images of oligodendrocytes cultured with DMSO (vehicle control), or one of three chemicals belonging to distinct hit categories identified by the primary screen, performed in one biological replicate. Nuclei are marked using DAPI and oligodendrocytes are marked using O1 . Scale bar, 50 μm. **d.** Primary chemical screen results displayed as viability normalized to DMSO. The solid line represents the average of the DMSO control (100%). The dotted line marks a reduction in viability of 30% (>3 SDs). The 206 cytotoxic hits that pass this threshold and were validated by MTS are colored in black. Non-cytotoxic chemicals and cytotoxic hits not validated by MTS are colored in gray. **e.** Characteristics of 49 oligodendrocyte-specific cytotoxic hits tested in 10-point dose response from (40

nM to 20 μM). IC_{50} values were determined with curve-fitting (nonlinear regression) and compared to median cytotoxicity values obtained from the EPA database for each chemical. Potency scores were calculated by dividing the cytotoxicity median by the experimentally determined IC_{50} in oligodendrocytes. Chemicals were ranked based on increasing potency score. Table also includes each chemical's use category. **f.** Chemotype analysis for the 49 oligodendrocyte-specific cytotoxic compounds, with the most enriched structural domain, bond.quatN_alkyl_acyclic (p-value = 0.002, OR = 16.2), highlighted in red. p-values were generated using a one-sided Fisher's exact test. **g.** Chemical structures for quaternary compounds. The enriched cytotoxicity-associated bond for quaternary ammonium compounds is highlighted in red. The quaternary phosphonium bond is highlighted in orange. **h-k.** Viability of oligodendrocytes, astrocytes, and fibroblasts treated with quaternary compounds, normalized to DMSO and IC_{50} determined by curve fitting. Data are presented as mean ± SEM, n = 3 biological replicates for each cell type.

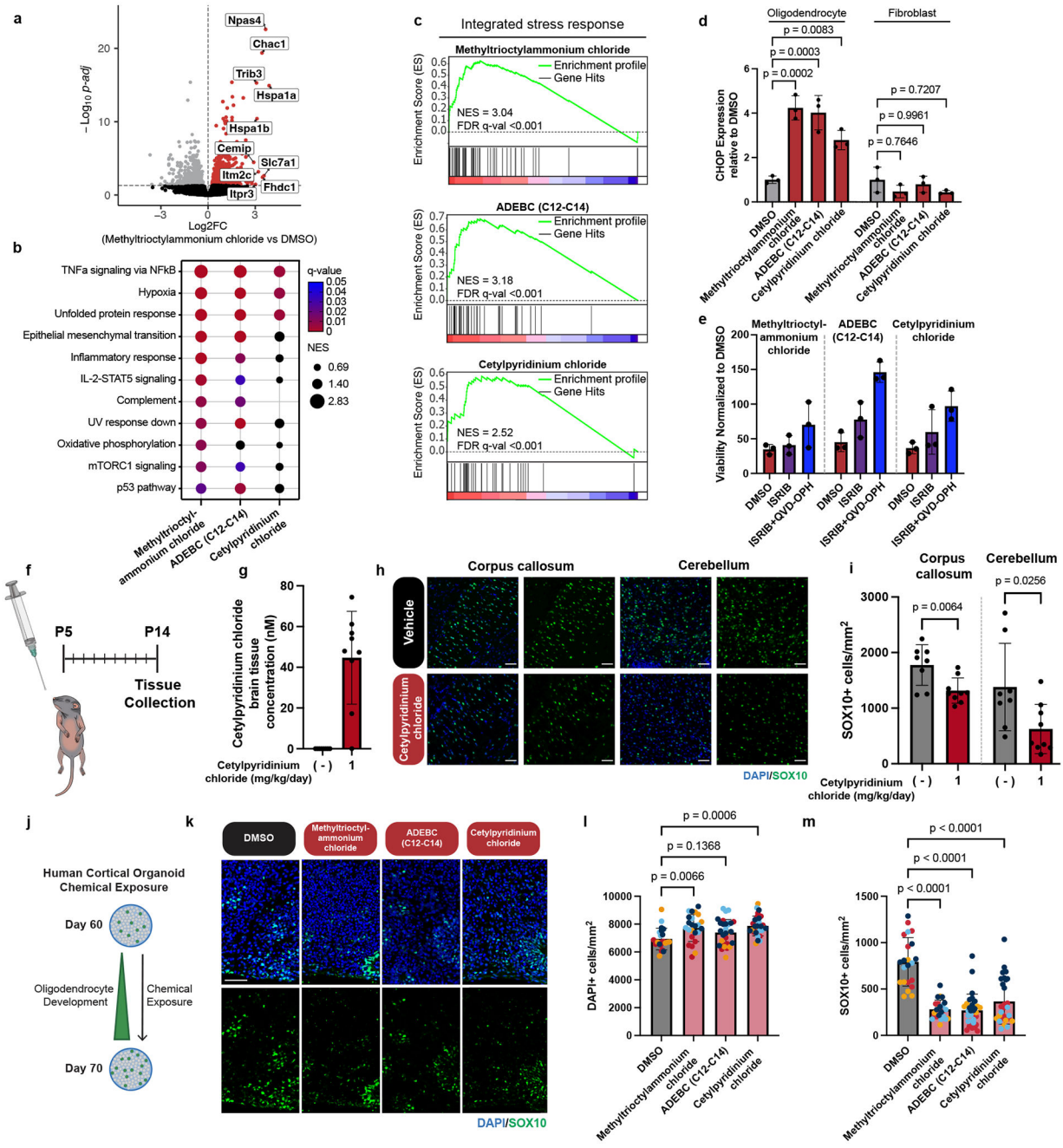

Fig. 2: Quaternary compounds activate the integrated stress response and are cytotoxic to human oligodendrocytes.

a-c. Oligodendrocytes were treated with quaternary compounds at IC_{75} (94 nM methyltrioctylammonium chloride, 370 nM ADEBC (C12-C14), and 181 nM cetylpyridinium chloride) for 4 hours. **a.** Volcano plot of differentially expressed genes after treatment with methyltrioctylammonium chloride. Genes in red increased (padj ≤ 0.05), as analyzed by DESeq2. Top 10 genes with the greatest log2FC are labelled. Gene set enrichment analysis (GSEA) of hallmark gene sets, with dots colored black

if q-value > 0.05 (**b**), and an integrated stress response gene set (**c**), n=3 biological replicates. **d.** qRT-PCR of CHOP in oligodendrocytes and fibroblasts treated with DMSO, or quaternary compounds at IC_{75}. Data are mean ± SD, n=3 biological replicates. p-values were calculated using one-way ANOVA with Dunnett post-test correction for multiple comparisons. Data for fibroblasts treated with additional concentrations are shown in Extended Data Fig. 2n. **e.** Oligodendrocyte viability normalized to DMSO after treatment with methyltrioctylammonium chloride, ADEBC (C12-C14), or cetylpyridinium chloride at IC_{75}, in combination with QVD-OPH (10 μM) and/or ISRIB (5 μM). Data are mean ± SD, n=3 biological replicates. **f-i.** Mice were gavaged daily with vehicle (water) or 1 mg/kg/day cetylpyridinium chloride from P5-P14. **f**. Schematic depicting delivery scheme. **g**. P14 cetylpyridinium chloride brain concentration, with analyte concentrations below the lower limit of detection (1 ng/mL) coded as 0. **h**. Representative images showing DAPI and SOX10 immunostaining. **i**. Quantification of SOX10+ oligodendrocytes in the corpus callosum and cerebellum. Data are mean ± SD, n=8 or 9 mice. p-values were calculated using an unpaired two-tailed t-test. **j-m.** Human cortical organoids were treated with DMSO, methyltrioctylammonium chloride, ADEBC (C12-C14), or cetylpyridinium chloride at IC_{75}. **j.** Schematic depicting 10-day treatment. **k**. Representative images showing DAPI and SOX10 immunostaining. Quantification of total cell number (DAPI+ per mm^2) (**l**) and oligodendrocytes (SOX10+ per mm^2) (**m**), in whole cortical organoids. Data are mean ± SD from n = 22, 24, 29, or 30 biological replicates (individual organoids generated from 4 independent batches). Individual data points are colored based on organoid batch. p-values were calculated using one-way ANOVA with Dunnett post-test correction for multiple comparisons (**l, m**). Scale bar, 50 μm (**h, k**).

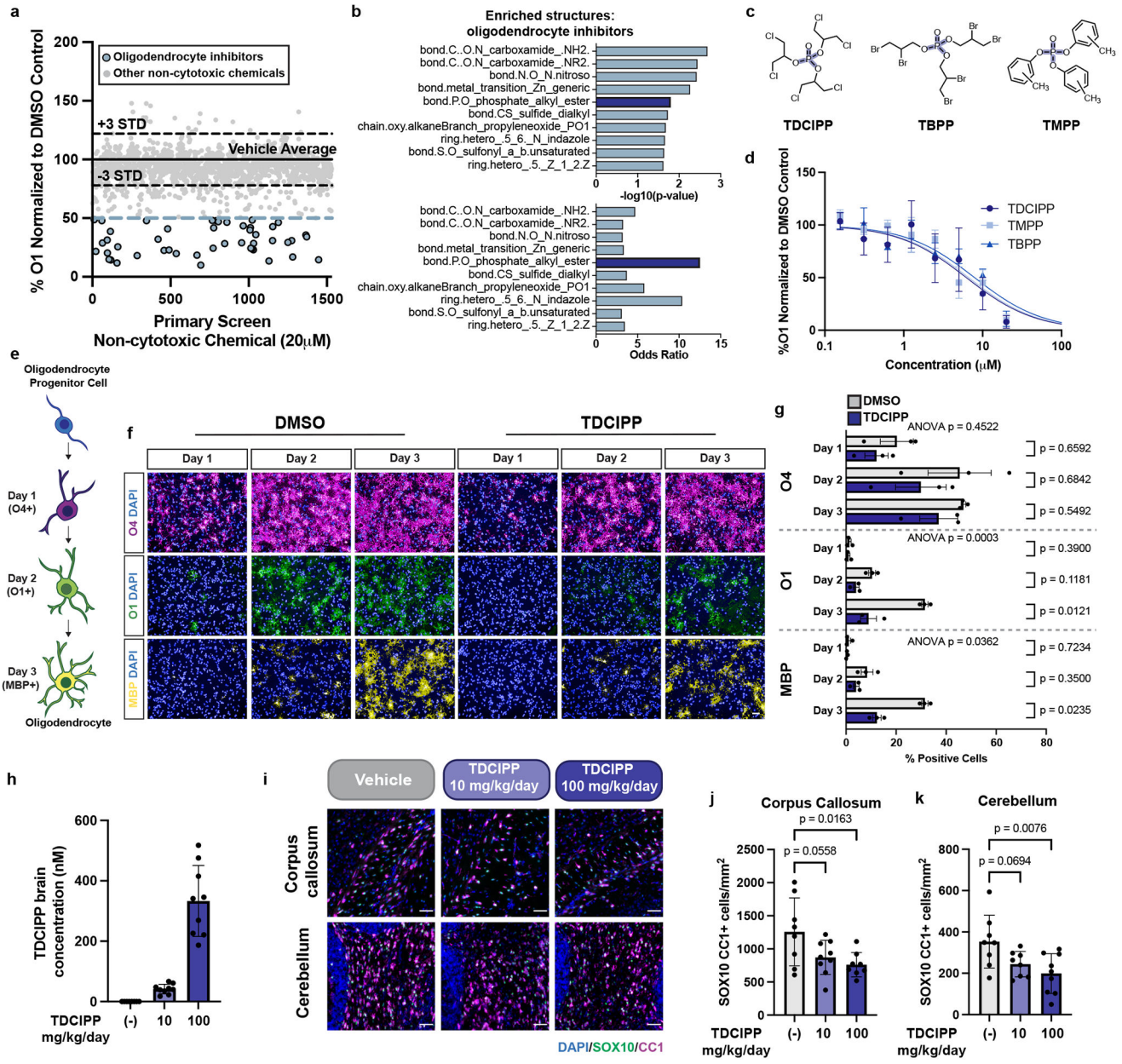

Fig. 3: Organophosphate flame retardants arrest oligodendrocyte maturation.

a. Primary chemical screen showing the effect of 1,531 non-cytotoxic environmental chemicals on oligodendrocyte development displayed as percent O1+ cells normalized to DMSO. Dotted lines mark ± 3 SDs. The blue dotted line marks the inhibitor hit cutoff, a reduction in O1+ cells of 50% (>7 SDs). The 47 oligodendrocyte inhibitors that pass this threshold are colored in blue. **b.** Chemotype analysis for oligodendrocyte inhibitors showing both the p-value and odds ratio. Among the top most significant structural domains, bond.P.O_phosphate_alkyl_ester (p-value = 0.02 , OR = 12.5) has the highest odds ratio, and is highlighted in dark blue. p-values generated using a one-sided Fisher's exact test. **c.** Chemical structures for three organophosphate flame retardants containing

the structure bond.P.O_phosphate_alkyl_ester, highlighted in blue. **d.** Percentage of (O1+) oligodendrocytes treated with organophosphate flame retardants normalized to DMSO. Data are mean ± SEM, n=3 biological replicates. **e.** Schematic showing stages of *in vitro* oligodendrocyte development and the markers for early (O4), intermediate (O1), and late (MBP) oligodendrocytes. **f-g.** Representative images (**f**) and quantification (**g**) of early (O4+), intermediate (O1+), and late (MBP+) oligodendrocytes after treatment with DMSO or 20 μM TDCIPP for 1, 2, and 3 days of maturation. Nuclei are marked using DAPI. Images and quantification for oligodendrocytes treated with TMPP and TBPP are shown in Extended Data Fig. 4e,f. Data are mean ± SEM, n=3 biological replicates. p-values were calculated using two-way ANOVA (ANOVA p =) for overall chemical differences with Dunnett's multiple comparison test for differences within each time point (p =). **h-k.** Mice were treated with vehicle (corn oil), 10 mg/kg/day, or 100 mg/kg/day TDCIPP from P5-P14. **h.** TDCIPP brain concentration at P14, analyte concentrations below the lower limit of detection (10 ng/mL) coded as 0. **i.** Representative images showing DAPI, SOX10, and CC1 immunostaining and quantification of SOX10+CC1+ oligodendrocytes in the cerebellum (**j**) and corpus callosum (**k**). Data are mean ± SD from n=8 or 9 mice. p-values calculated using one-way ANOVA with Dunnett post-test correction for multiple comparisons. Scale bar, 50 μm (**f, i**).

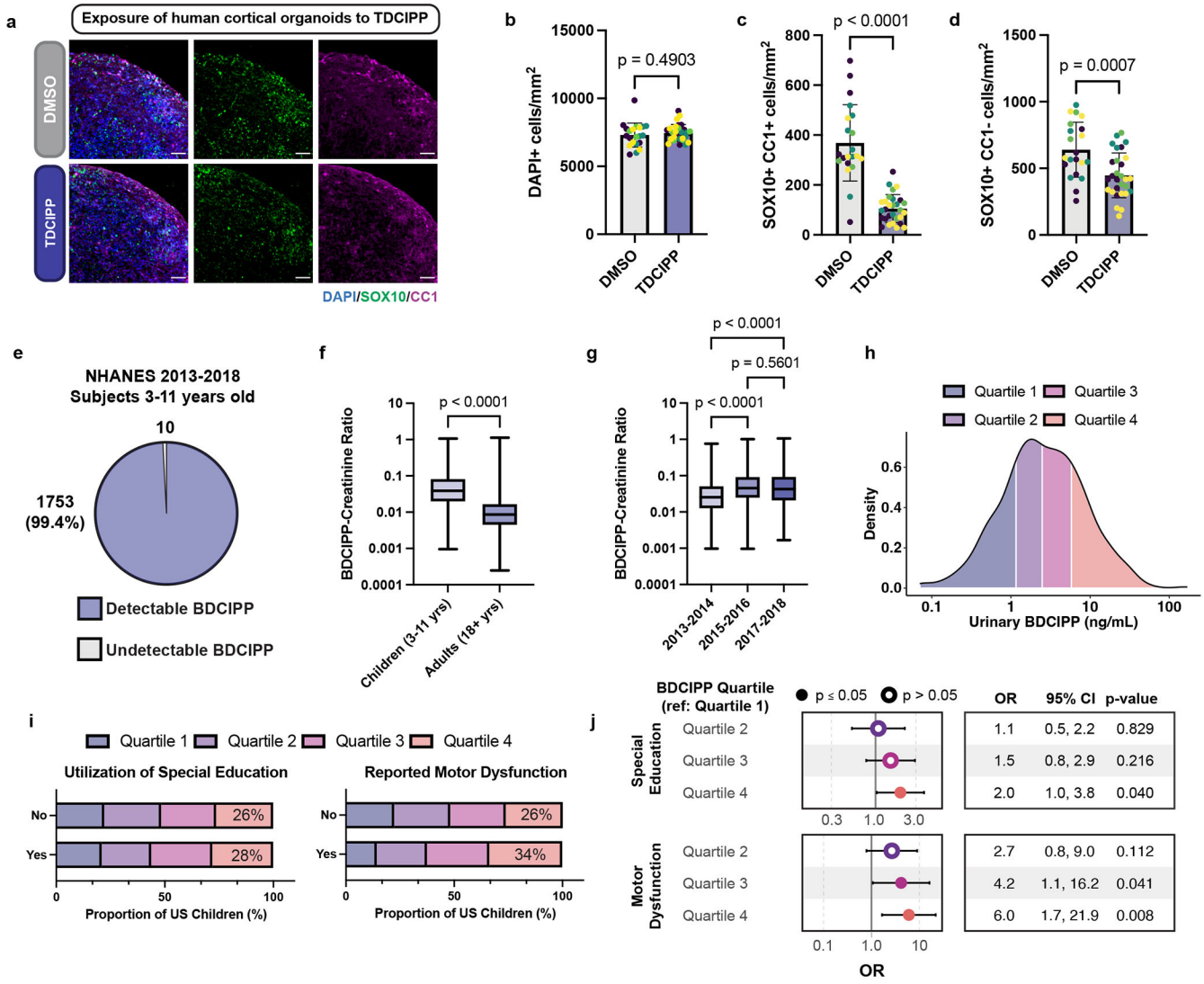

Fig. 4: TDCIPP inhibits human oligodendrocyte development and is associated with abnormal neurodevelopmental outcomes in children.

a-d. Human cortical organoids were treated with DMSO or TDCIPP at IC_{75} (18.7 μM). **a**. Representative images of human cortical organoids showing DAPI, SOX10, and CC1 immunostaining. Scale bars, 50 μm. Quantification total cell number (DAPI+ per mm^2) (**b**), oligodendrocytes (SOX10+CC1+ per mm^2) (**c**), and oligodendrocyte progenitors (SOX10+CC1− per mm^2) (**d**), in whole cortical organoids. Data are mean ± SD, n = 21 or 29 biological replicates (individual organoids generated from 4 independent batches). Data points are colored based on organoid batch. p-values were calculated using unpaired two-tailed t test. **e.** Pie chart showing the number of children ages 3-11 years old from the NHANES 2013-2014, 2015-2016, and 2017-2018 datasets with undetectable and detectable levels of BDCIPP, the urine metabolite of TDCIPP. **f.** Creatinine-normalized levels of BDCIPP in children (3-11 years old), n = 1762, and adults (>18 years), n = 4988. p-value calculated using the two-sided Mann-Whitney U-test. **g.** Creatinine-normalized levels of BDCIPP in children 3-11 years of age across three NHANES data cycles, n = 337,

675 or 749. p-values were calculated using the Kruskal-Wallis test with Dunn's multiple comparisons test. **h.** Range and quartiles of urine BDCIPP levels in children ages 3-11 years old from the NHANES 2013-2014, 2015-2016, and 2017-2018 datasets. **i.** Proportions of all US children in each urinary BDCIPP quartile, who utilize special education or have motor dysfunction. **j**. Fully adjusted odds ratio for the neurodevelopmental outcomes: special education and motor dysfunction, n = 1564 or 1566. Significant odds ratios (p-value ≤ 0.05) are indicated by closed circles (BDCIPP Q4 v Q1 OR 2.0 [95% CI = 1.0-3.8] for special education; BDCIPP Q3 v Q1 OR 4.2 [95% CI = 1.1-16.2], and BDCIPP Q4 v Q1 OR 6.0 [95% CI = 1.7-21.9] for motor dysfunction). Closed and open circles are the odds ratio and error bars indicate the 95% CI. Odds ratios and p-values were using the "survey" and "gtsummary" R packages. The Wald test was used to calculate p-values. Data for odds ratios and p-values calculated for all covariates are shown in Extended Data Fig. 5 d,e.